AN ABSTRACT OF THE THESIS OF

DAVID MERLE BARNHART for the Ph. D. in Chemistry
(Name) (Degree) (Major)

Date thesis is presented May 15, 1964

Title THE EFFECT OF TEMPERATURE ON THE MOLECULAR STRUCTURE OF GASEOUS ARSENIC TRIBROMIDE.

Redacted for Privacy

Abstract approved
(Major professor)

The molecular structure of arsenic tribromide has been studied by electron diffraction from the vapor at nozzle temperatures of 370° K and 473° K. The root-mean-square amplitudes of vibration were found to be significantly greater at the higher temperature. The increases were 15 and 19 percent for l_{As-Br} and $l_{Br...Br'}$ respectively, in good agreement with prediction from simple theory. The results for the interatomic distances, root-mean-square amplitudes, and the bond angle $\angle$Br-As-Br at 370° K and 473° K, respectively, are $r_{As-Br} = 2.329 \pm 0.002$ Å and 2.331 ± 0.002 Å; $r_{Br...Br} = 3.561 \pm 0.005$ Å and 3.563 ± 0.005 Å; $l_{As-Br} = 0.047_9 \pm 0.004_5$ Å and $0.055_5 \pm 0.004_5$; $l_{Br...Br} = 0.113_2 \pm 0.005_3$ Å and $0.135_3 \pm 0.005_3$ Å; and $\angle$Br-As-Br = $99.6_6 \pm 0.2_6°$ and $99.7_2 \pm 0.2_9°$. These values were determined from least-squares refinements of intensity curves. The estimated standard errors

include standard deviations derived from the least-squares procedure, estimates of correlation among the data, uncertainties in the constants of the experiment, and uncertainties in the factors employed in data reduction.

Using the mean-square amplitudes of vibration obtained from the electron diffraction experiments together with the normal vibration frequencies, a set of values has been derived for the potential constants of a general quadratic vibrational potential function. The values in millidynes/Å are $f_r = 1.69$, $f_{rr} = 0.23$, $f_R = 0.42$, $f_{RR} = 0.07$, $f_{rR} = -0.07$; $f'_{rR} = -0.05$. These results suggest that a simple central force field can be applied with confidence to arsenic tribomide

THE EFFECT OF TEMPERATURE ON THE MOLECULAR STRUCTURE OF GASEOUS ARSENIC TRIBROMIDE

by

DAVID MERLE BARNHART

A THESIS

submitted to

OREGON STATE UNIVERSITY

in partial fulfillment of
the requirements for the
degree of

DOCTOR OF PHILOSOPHY

June 1964

APPROVED:

Redacted for Privacy

Associate Professor of Chemistry

In Charge of Major

Redacted for Privacy

Chairman of Department of Chemistry

Redacted for Privacy

Dean of Graduate School

Date thesis is presented _____

Typed by Nancy Kerley

ACKNOWLEDGMENTS

My sincere thanks go to Dr. Kenneth Wayne Hedberg for his guidance and direction in the planning and interpretation of this investigation.

This thesis is dedicated

To My Wife

TABLE OF CONTENTS

LIST OF TABLES

LIST OF TABLES (continued)

LIST OF FIGURES

THE EFFECT OF TEMPERATURE ON THE STRUCTURE OF GASEOUS ARSENIC TRIBROMIDE

INTRODUCTION

The effect of molecular vibrations on the intensity of x-rays scattered by free molecules was first investigated by James (27, p. 737-754). His treatment yields a result which is also applicable to electron scattering, and over the years has been repeatedly employed in structure determinations by electron diffraction, largely to bring about better agreement between the calculated and observed scattered intensities.

A natural application of James' theory would appear to concern a determination of the form and amplitudes of molecular vibrations instead of a simple taking into account of their effect on the scattered intensity, and this has been done in a few cases (22, p. 589-594; 34, p. 643-652). The procedure is straight-forward in concept. According to James, assuming harmonic vibrations, the scattered intensity from each atomic pair includes a factor

$$A(s) = \exp(-2^{-1}\ \delta\overline{l_{ij}^2}s^2\ ) \qquad (1)$$

where δl_{ij}^2 is the mean-square-amplitude of vibration associated with atom pair i, j and $s = 4\pi\lambda^{-1}\sin\Theta$ is dependent on the wavelength of the electrons and on the scattering angle 2Θ. Now, if $\mathbf{U}$ denotes the transformation matrix for the transformation of normal coordinates, $\mathbf{Q}$, to internuclear displacement coordinates, Δr,

(internal coordinates), the matrix of mean square amplitudes of vibration is given by (33, p. 1927)

$$\mathbf{\Sigma}_r = \langle \mathbf{\Delta r}\ \mathbf{\Delta r}' \rangle = \mathbf{U \Delta U}' \tag{2}$$

$\mathbf{\Delta}$ is a diagonal matrix whose elements (for harmonic vibrations) are (8, p. 295)

$$\Delta_i = \langle Q_i^2 \rangle = \frac{h}{8\pi^2 \nu_i} \coth \frac{h\nu_i}{2kT} \tag{3}$$

where Q_i is the ith normal coordinate, ν_i the normal frequency, h Planck's constant, k Boltzmann's constant and T the absolute temperature. It has been shown (13, p. 1121) that in the classical limit, that is for high temperatures and low frequencies, the mean square amplitudes are linearly related to the temperature: under these conditions

$$h\nu_i / 2kT << 1 \tag{4}$$

and

$$\coth h\nu_i / 2kT = 2kT / h\nu_i \tag{5}$$

from which is obtained

$$\Delta_i = k\lambda_i^{-1} T \tag{6}$$

$$\mathbf{\Delta} = kT\mathbf{\Lambda}^{-1} \tag{7}$$

$$\mathbf{\Sigma}_r = kT\, \mathbf{U \Lambda}^{-1} \mathbf{U}' \tag{8}$$

where

$$\lambda_i = (4\pi^2 \nu_i^2) \ .$$

Thus, the diagonal elements of the matrix, which are the observed

mean-square-amplitudes, are proportional to absolute temperature, and an increase of 100° C at room temperature would predict an increase of about 13 percent in the root-mean-square amplitude of vibration. Since the errors associated with these parameters are about one-third of this increase, significant measurements should be, and have proven to be (in the case of phosphorus trichloride (22, p. 589-594)), easy. An investigation of this "temperature effect," in the case of arsenic tribromide, constitutes a part of this thesis work.

Of more interest than the demonstration of a temperature effect is the question of a determination of the intramolecular potential function, which may be expressed in the harmonic oscillator approximation by

$$2V = \sum_{k,l} f_{k,l} q_l q_k \qquad (9)$$

where the q_i's are some set of molecular coordinates, and the $f_{k,l}$'s are "potential constants." The connection between these $f_{k,l}$'s and equation (2) may be seen by the following: If the q_i's of equation (9) are the internal coordinates of equation (2), equation (9) may be written as

$$2V = \mathbf{Q}' \mathbf{U}' \mathbf{F}_r \mathbf{U} \mathbf{Q} \quad . \qquad (10)$$

It is well-known (38, p. 309) that $\mathbf{U}$ is chosen such that

$$\mathbb{U}' \mathbb{F}_r \mathbb{U} = \mathbb{\Lambda} \tag{11}$$

Therefore, by substituting equation (11) in equation (8) the diagonal elements of the $\mathbb{\Sigma}_r$ matrix may be expressed in terms of the $f_{k,l}$'s.

Knowledge of the vibrational potential function is of great importance in interpreting chemical and physical properties of molecules in terms of their structures, and is a great aid to spectroscopists in assigning the observed vibrational frequencies (in infrared and raman experiments) to the normal modes of vibration. Spectroscopists are handicapped in this task since there are usually more such constants than observable frequencies (15, p. 511). The additional experimental evidence provided by electron diffraction allows, then, for a determination of a more general potential function.

There exists another approach to the vibrational potential function problem, this being through the inverse $\mathbb{F}$ matrix, or "compliance matrix" (14, p. 241-248). Since

$$\mathbb{F}_r^{-1} = \mathbb{U}\mathbb{\Lambda}^{-1}\mathbb{U}' \tag{11a}$$

Equation (8) may be written as

$$\mathbb{\Sigma}_r = kT\,\mathbb{F}_r^{-1} \tag{8a}$$

or letting $\mathbb{C} = \mathbb{F}^{-1}$

$$\mathbb{\Sigma}_r = kT\,\mathbb{C}_r \tag{8b}$$

Although complete knowledge of $\mathbb{C}$ implies knowledge of $\mathbb{F}$ through the inverse transformation, there is a certain usefulness to the compliance matrix approach. As mentioned above, the solution of the potential problem may be handicapped by lack of sufficient experimental data. Further, $\mathbb{F}$ may be determined only if $\mathbb{F}^{-1}$ is known completely. Equation (8b) shows that the major diagonal compliance constants, which are related to the bonded and non-bonded distances in the molecule, can be obtained without complete determination of all the constants. The units of $\mathbb{F}$ are millidynes per angstrom, that is, the force necessary to produce a unit change in distance, and the units of $\mathbb{C}$ are angstroms per millidyne, or the change in distance produced by a unit force. Knowledge of either the compliance or force constant for a given bond, for example, implies the same knowledge of that bond's strength. Therefore, when the problem is not completely solvable, the determination of the compliance constants from equation (8b) for the bonded and non-bonded distances may prove useful in structural analyses.

The mean-square-amplitudes of arsenic tribromide, along with the vibrational frequencies from raman spectroscopy, were used as part of this thesis work to determine the potential function of the molecule. Both the compliance constant and the potential constant approach have been employed.

The choice of arsenic tribromide as an example for study was

based on several considerations. First, the simple structure of the molecule with two widely separated internuclear distances promised high accuracy in the values of the determined parameters and a minimum of correlation among errors. Second, the complicating effect of phase shift (19, p. 669) is minimized by the small atomic number difference. Third, the molecule has four active vibrational frequencies which, with the two mean-square amplitudes, provides sufficient information to attempt the determination of the six potential constants associated with the general quadratic potential function for the molecule (23, p. 596).

EXPERIMENTAL

Although the technique of molecular structure determination by gaseous electron diffraction has been described in other theses (10, p. 5-44; 35, p. 63-116), there exist certain differences between the earlier work and the work to be described here, which makes a moderately detailed account of the latter desirable. These differences are due partly to the apparatus used and include somewhat different data reduction procedures.

The electron diffraction photographs of arsenic tribromide were taken at the University of Oslo, Norway. (Other work at Oregon State University has been based on data from the California Institute of Technology.) The Oslo apparatus has been described by Bastiansen, Hassel and Risberg (4, p. 232-238). A simplified diagram of this apparatus is shown in Figure 1a. Its principal difference from the California apparatus is its larger size, which gives an extended range of scattering angles by allowing a variable camera distance and permits greater flexibility with auxillary units. The electron source is a hot cathode electron gun (A) from a commercial electron microscope, mounted above the focusing device, a magnetic lens (B). Gas is released through a nozzle (C) and frozen out on a cold trap (D) opposite the nozzle. An enlarged view of the nozzle and cold trap is shown in Figure 1b. The well-collimated

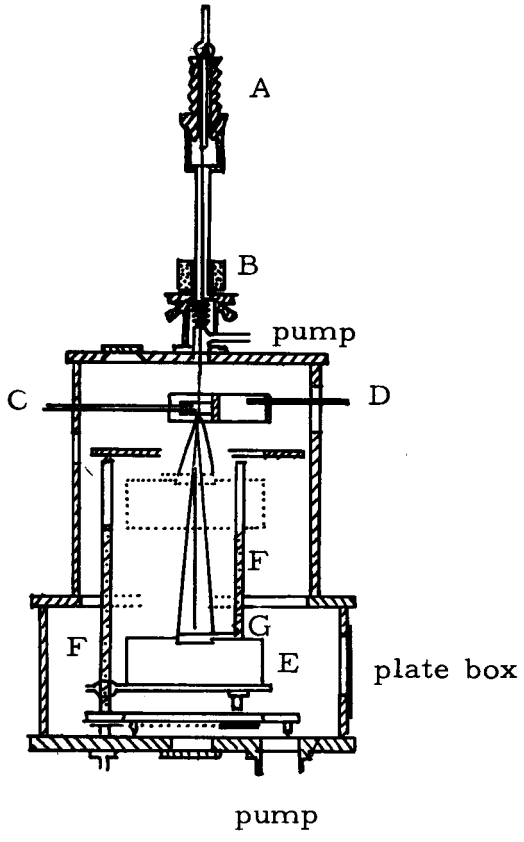

FIGURE 1a. Simplified Section Sketch of the Oslo Electron Diffraction Apparatus.

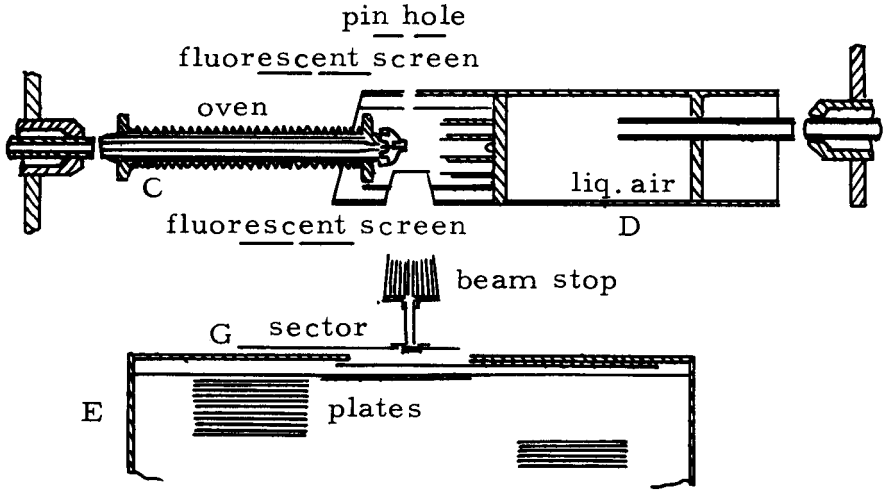

FIGURE 1b. Enlarged Detail Sketches of the Plate Box and Nozzle Assembly for the Oslo Electron Diffraction Apparatus.

electron beam is diffracted by the gas and the scattered radiation detected by photographic plates at (E). A number of plates may be positioned for exposure during one experiment as is shown in Figure 1b. The plate box may be translated in the vertical direction (a second position is shown by the dotted lines) by means of chain-driven screws (F, Figure 1a) which carry the plate box support. The apparatus also uses a spiral shaped sector (G, Figure 1b) rotated during exposure about the axis of the undiffracted beam; the sector opening is an increasing function of the scattering angle and prevents overexposure of the plates at small angles (11, p. 404-406).

A commercial sample (CIBA) of arsenic tribromide of high purity (99+ percent) was used without purification. Diffraction photographs were taken at two temperatures (370° K and 473° K) using Kodak process plates. Early attempts at higher temperatures (above 573° K) resulted in decomposition of the sample. The temperature 473° K was the highest attainable without significant sample decomposition, as ascertained by separate experiments in which arsenic tribromide was heated in the presence of metal of the same kind as encountered in the heated nozzle.

Two camera distances were used at each of the two temperatures. These were 47.85 centimeters and 19.15 centimeters at 370° K and 48.21 centimeters and 19.53 centimeters at 473° K. Five photographs were selected for analysis from the low temperature

long-camera-distance experiment and four at the short camera distance. The same number of plates were selected at the corresponding distances at the high temperature.

The electron wave lengths were determined in separate experiments on thin gold foil (9, p. 242). They were found to be 0.06461 Angstroms at the lower temperature and 0.06454 Angstroms at the higher.

DATA REDUCTION

A photographic plate from the long camera distance at the high temperature is reproduced in Figure 2. The plate shows a series of concentric, diffuse rings superimposed on a smooth, declining background, the blackness (density) of the plate being approximately proportional to the intensity of the scattered radiation striking the plate. The first step in the data reduction procedure was to obtain a precise functional relationship between this blackness, or photographic density, and the intensity of the scattered electrons striking the photographic plate, I_p. The second step was the calculation of the total intensity function, I_t, from I_p: I_t contains the molecular scattering function needed in the structure determination. The final step in the data reduction consists of separating the molecular scattering function from the total intensity.

The photographic density was measured with a Leeds and Northrup recording microdensitometer. This instrument consists essentially of an optical system which includes the light source, focusing lenses and photocell, and a table with its surface perpendicular to the light beam, which can be driven at selected constant speeds through the light beam. The photographic plate is placed on an oscillating mechanism which is mounted on the table (29, p. 765). The plate is oscillated about the axis of the diffraction rings during

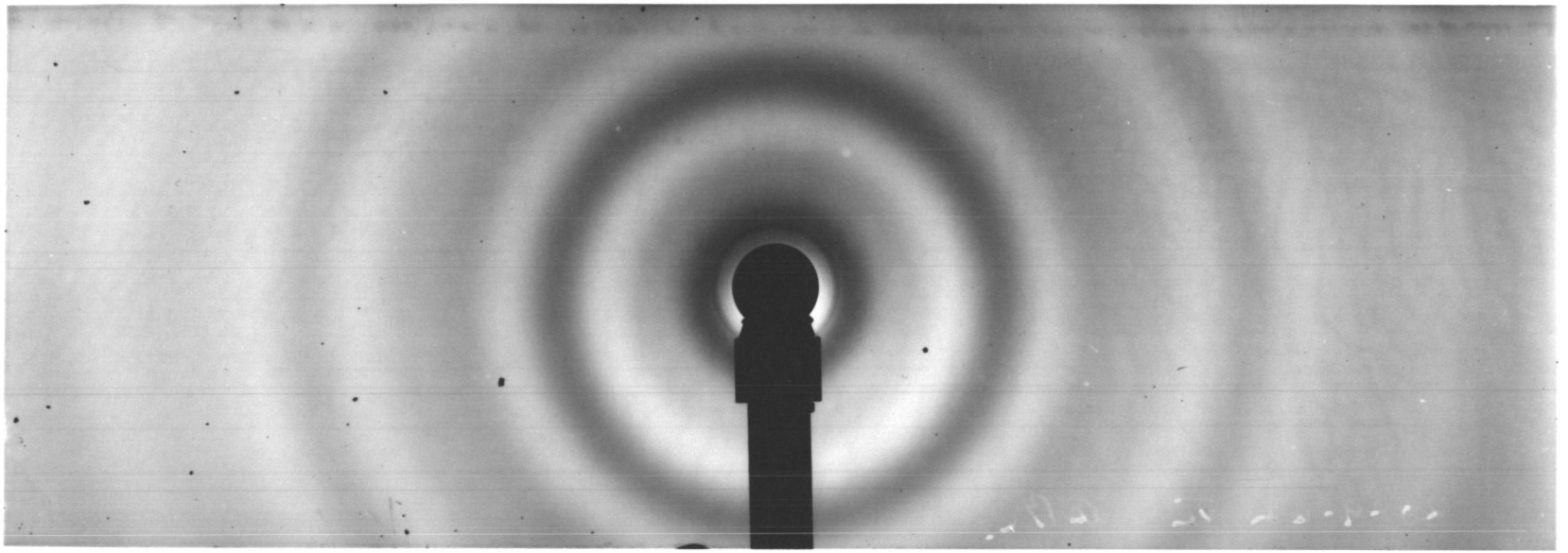

FIGURE 2. Electron Diffraction Photograph of Arsenic Tribromide.

photometry in order to even out the graininess of the emulsion while being carried through the light beam. The light transmitted by the plate is detected by the photo cell from which an amplified signal is taken to operate the pen of a strip chart recorder. In Figure 3 one such trace is reproduced. Each trace consists of two "branches" corresponding to the right and left sides of the photographic plate with the undiffracted beam position as center. Traces were made with the two edges of the chart paper recording, as nearly as possible, 0 percent and 100 percent absorption of the densitometer beam by the plate. This was a matter of adjusting the zero (null) point and the amplification of the instrument. The plates were first passed through the beam at the rate of 50 millimeters per minute which, with the standard chart speed used, gave a 5.24:1 ratio of the position coordinate. The plates were then re-traced, reducing the plate translation speed to 10 millimeters per minute to give an expanded scale on the trace; this expanded scale made more convenient the reading of data from the trace. Many of the plates had a rather heavy background and, consequently, a high average density. Under these conditions the fluctuations of density, which contain the molecular structure dependent information, are very small on the intensity scale 0 - 100 percent absorption, corresponding to the full width of the strip chart. Accordingly, these second tracings were run with a more intense ("amplified") photometer beam. The effect of this may be easily

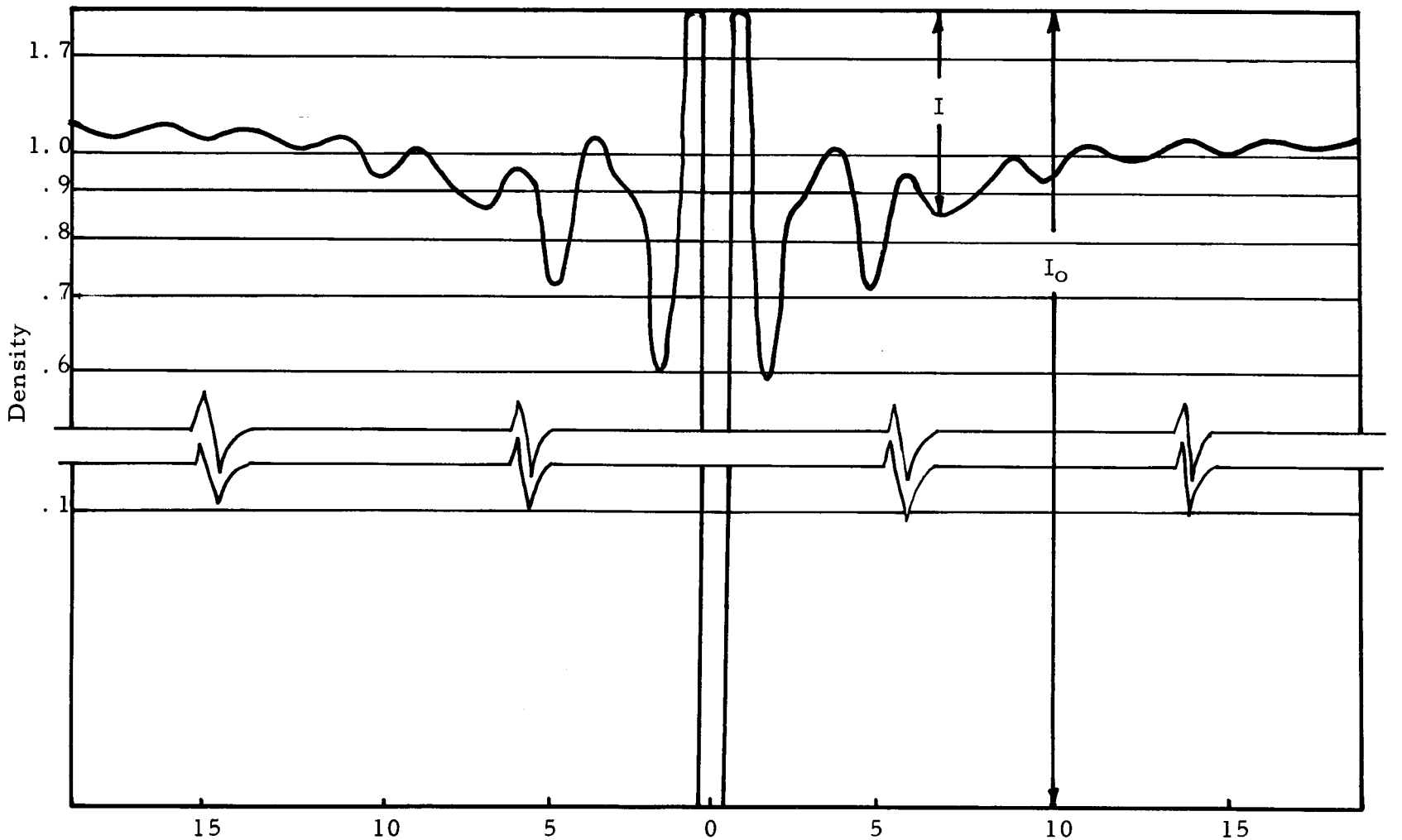

FIGURE 3. Typical Photometer Trace of Photographic Plates. Scale in s Units.

visualized by regarding the amplification as a displacement of the zero percent absorption point from the edge of the strip chart to some (to be determined) point off the chart, with corresponding amplification of the molecular structure sensitive fluctuations.

If I and I' denote the intensities of the densitometer beam transmitted by the photographic plate for the unamplified and amplified cases respectively, and I_o, I'_o the corresponding 100 percent transmission intensities, then the readings taken from corresponding points of the two traces allow calculation of optical densities by

$$D_i = k \log \frac{I^o}{I_i} \tag{12}$$

and

$$D_i = k \log \frac{I^{o'}}{I_i'} \tag{13}$$

For reasons given above, I' is more accurately measured than is I, so that D is most advantageously calculated from equation (13). This necessitates a determination of $I^{o'}$ which may be done as follows. From equation (13) one has

$$D_i = k \log \frac{I^{o'}}{I_i'} = k \log \frac{I^o}{I_i'} + k \log \frac{I^{o'}}{I^o} \tag{14}$$

For corresponding points on the two traces the right-hand sides of equations (12) and (13) may be equated giving

$$\log \frac{I^{o'}}{I_i'} = \log \frac{I^o}{I_i} \tag{15}$$

or

$$\log \frac{I^{o'}}{I^{o}} = \log \frac{I_i'}{I_i} \tag{16}$$

Equation (16) may be substituted into equation (14) giving

$$\log \frac{I^{o'}}{I_i'} = \log \frac{I^{o}}{I_i'} + \log \frac{I_i'}{I_i} \tag{17}$$

The desired readings (the left-hand side of equation 17) are thus obtained from the readings actually made (the first term on the right) by adding a correction constant (the second term on the right), the latter being obtained by averaging, say, several readings I_i'/I_i of corresponding, convenient points, i, such as well-defined maxima or minima from the amplified and unamplified traces.

It is convenient to read values D_i from the traces at an interval $s = \frac{1}{4}$ (s has been defined on page 1) or some whole number multiple of the interval. s-scales were prepared by first calculating Θ_i for each value of s, then calculating the corresponding radial distance on the plate (x_p) from $x_p = L \tan \Theta$ where L is the perpendicular distance from the plate to the scattering point, and, finally, converting x_p to x_T (radial distance on the trace) by use of the ratio x_p/x_T established by making a microdensitometer trace of a calibrated glass scale.

The response of photographic plates is not linear with exposure to electrons over all exposure ranges and curves known as "blackness correction" curves must be prepared to correct densities

TABLE 1. s-Scales (in cm).

	370°K		473°K			370°K		473°K	
s	48 cm	19 cm	48 cm	19 cm	s	48 cm	19 cm	48 cm	19 cm
.00	0.00		0.00		10.00	25.90	10.37	26.03	10.55
.25	0.65		0.65		10.25	26.56	10.63	26.69	10.81
.50	1.29		1.30		10.50	27.21	10.89	27.34	11.08
.75	1.94		1.95		10.75	27.87	11.15	28.00	11.34
1.00	2.58		2.59		11.00	28.52	11.41	28.66	11.61
1.25	3.23		3.24		11.25	29.17	11.67	29.32	11.88
1.50	3.87		3.89		11.50	29.83	11.94	29.97	12.14
1.75	4.52		4.54		11.75	30.48	12.20	30.63	12.41
2.00	5.16		5.10		12.00	31.14	12.46	31.29	12.68
2.25	5.81		5.84		12.25	31.79	12.72	31.95	12.95
2.50	6.45		6.48		12.50	32.45	12.99	32.61	13.21
2.75	7.10		7.13		12.75	33.11	13.25	33.27	13.48
3.00	7.74		7.78		13.00	33.77	13.51	33.93	13.75
3.25	8.39		8.43		13.25	34.42	13.78	34.60	14.02
3.50	9.03		9.08		13.50	35.08	14.04	35.26	14.28
3.75	9.68		9.73		13.75	35.74	14.31	35.92	14.55
4.00	10.33		10.38		14.00	36.40	14.57	36.58	14.82
4.25	10.97		11.03		14.25	37.06	14.83	37.25	15.10
4.50	11.62		11.68		14.50	37.72	15.10	37.91	15.36
4.75	12.27		12.33		14.75	38.39	15.36	38.58	15.63
5.00	12.91	5.17	12.98	5.26	15.00	39.05	15.63	39.24	15.90
5.25	13.56	5.43	13.63	5.52	15.25	39.71	15.89	39.91	16.17
5.50	14.21	5.69	14.28	5.78	15.50	40.38	16.16	40.58	16.44
5.75	14.85	5.94	14.93	6.05	15.75	41.04	16.42	41.24	16.71
6.00	15.50	6.20	15.58	6.31	16.00	41.70	16.69	41.91	16.98
6.25	16.15	6.46	16.38	6.58	16.25	42.37	16.96	42.58	17.25
6.50	16.80	6.72	16.88	6.84	16.50	43.04	17.22	43.25	17.52
6.75	17.45	6.98	17.53	7.10	16.75	43.70	17.49	43.92	17.79
7.00	18.09	7.24	18.18	7.37	17.00	44.37	17.76	44.59	18.06
7.25	18.74	7.50	18.84	7.63	17.25	45.04	18.02	45.26	18.34
7.50	19.39	7.76	19.49	7.90	17.50	45.70	18.29	45.93	18.61
7.75	20.04	8.02	20.14	8.16	17.75	46.38	18.56	46.60	18.88
8.00	20.69	8.28	20.79	8.43	18.00	47.04	18.83	47.28	19.15
8.25	21.34	8.54	21.45	8.69	18.25	47.72	19.10	47.95	19.43
8.50	21.99	8.80	22.10	8.95	18.50	48.39	19.36	48.63	19.70
8.75	22.64	9.06	22.76	9.22	18.75	49.06	19.63	49.30	19.97
9.00	23.29	9.32	23.41	9.48	19.00	49.73	19.90	49.98	20.25
9.25	23.95	9.58	24.06	9.75	19.25	50.41	20.17	50.66	20.53
9.50	24.60	9.84	24.72	10.02	19.50	51.08	20.44	51.34	20.80
9.75	25.25	10.10	25.38	10.28	19.75	51.76	20.71	52.01	21.07

TABLE 1. Continued.

	370°K		473°K			370°K		473°K	
s	48 cm	19 cm	48 cm	19 cm	s	48 cm	19 cm	48 cm	19 cm
20.00		20.98		21.35	30.00		32.13		32.69
20.25		21.25		21.62	30.25		32.42		32.98
20.50		21.53		21.90	30.50		32.71		33.28
20.75		21.80		22.18	30.75		33.00		33.57
21.00		22.07		22.45	31.00		33.29		33.86
21.25		22.34		22.73	31.25		33.58		34.16
21.50		22.61		23.00	31.50		33.87		34.46
21.75		22.89		23.29	31.75		34.16		34.75
22.00		23.16		23.56	32.00		34.45		35.05
22.25		23.43		23.84	32.25		34.75		35.35
22.50		23.71		24.12	32.50		35.04		35.65
22.75		23.98		24.40	32.75		35.33		35.95
23.00		24.26		24.68	33.00		35.63		36.24
23.25		24.53		24.96	33.25		35.92		36.55
23.50		24.81		25.24	33.50		36.22		36.85
23.75		25.09		25.52	33.75		36.52		37.15
24.00		25.36		25.80	34.00		36.81		37.45
24.25		25.64		26.08	34.25		37.11		37.75
24.50		25.92		26.37	34.50		37.41		38.06
24.75		26.19		26.65	34.75		37.71		38.36
25.00		26.47		26.93	35.00		38.00		38.66
25.25		26.75		27.22	35.25		38.31		38.97
25.50		27.03		27.50	35.50		38.61		39.28
25.75		27.31		27.78	35.75		38.91		39.58
26.00		27.59		28.07	36.00		39.21		39.89
26.25		27.87		28.35	36.25		39.52		40.20
26.50		28.15		28.64	36.50		39.82		40.51
26.75		28.43		28.92	36.75		40.12		40.82
27.00		28.71		29.21	37.00		40.43		41.13
27.25		29.00		29.50	37.25		40.74		41.44
27.50		29.28		29.79	37.50		41.04		41.75
27.75		29.56		30.01	37.75		41.35		42.06
28.00		29.84		30.36	38.00		41.66		42.38
28.25		30.13		30.65	38.25		41.97		42.69
28.50		30.41		30.94	38.50		42.28		43.01
28.75		30.70		31.23	38.75		42.59		43.32
29.00		30.98		31.52	39.00		42.90		43.64
29.25		31.27		31.81	39.25		43.21		43.96
29.50		31.56		32.10	39.50		43.52		44.27
29.75		31.84		32.40	39.75		43.84		44.59

not within the linear response range of the plates. A typical curve is shown in Figure 4. It may be constructed by a method due to Karle and Karle (28, p. 958) which involves forming ratios of densities taken from corresponding points of traces from a light and a heavy plate. These ratios will be constant so long as the densities taken point by point from each plate are light enough to fall on the linear part of the density-exposure response curve. Since the densities of each plate change in a more or less monotonous manner as a function of radial distance, the set of ratios mentioned above will gradually begin to deviate from constancy as the measured densities gradually increase: those taken from the heavier plate begin to fall on the non-linear part of the density-exposure curve while the corresponding points taken from the light curve still fall on the linear part. The change in the ratio of densities may thus be used to correct the measured densities of the heavier plate. For a number of reasons related to the exposure ranges of the arsenic tribromide plates, it turned out to be inconvenient to use them in derivation of the curve. Instead, diffraction patterns from gold foil were used for this purpose. Also used was the standard correction curve employed by the Oslo group. This curve is a composite of results from many experiments on different gas molecules. There were some differences between the gold foil derived blackness correction curve and the Oslo curve; the effect of these differences will be discussed later.

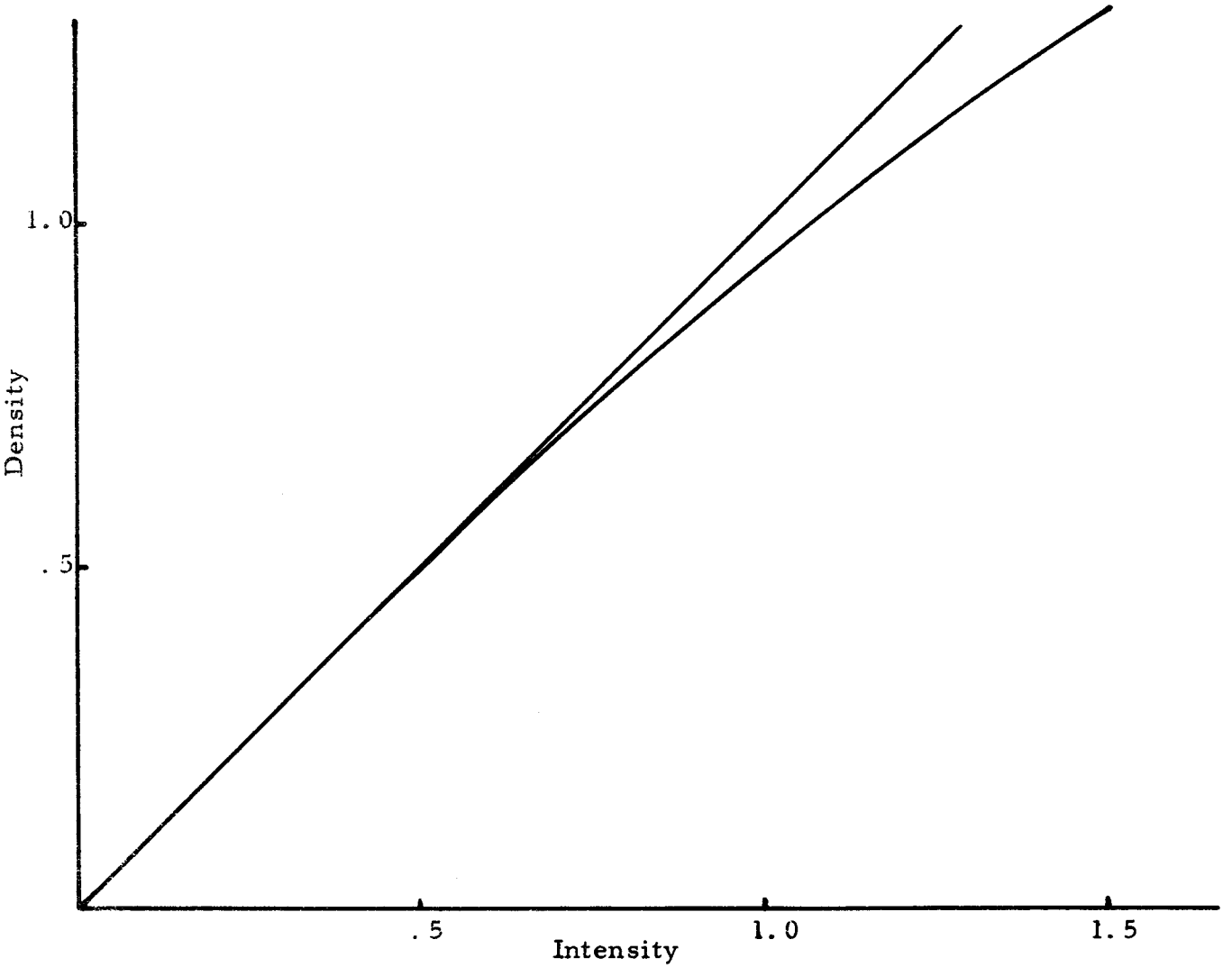

FIGURE 4. A Typical Blackness Correction Curve (Constructed from Gold Foil Diffraction Photographs).

TABLE 2. Blackness Correction Tables.

Density	ΔI_O	$\Delta I_{GF}^{370^\circ K}$	$\Delta I_{GF}^{473^\circ K}$	Density	ΔI_O	$\Delta I_{GF}^{370^\circ K}$	$\Delta I_{GF}^{473^\circ K}$
.50	.000	.000	.000	1.50	.298	.191	.303
.52	.000	.000	.002	1.52	.312	.202	.315
.54	.000	.000	.003	1.54	.325	.214	.326
.56	.000	.000	.005	1.56	.339	.228	.339
.58	.000	.001	.007	1.58	.353	.242	.351
.60	.000	.001	.010	1.60	.367	.257	.365
.62	.000	.002	.012	1.62	.382	.271	.379
.64	.000	.003	.014	1.64	.397	.285	.393
.66	.001	.005	.016	1.66	.412	.300	.407
.68	.001	.006	.018	1.68	.427	.315	.422
.70	.002	.008	.022	1.70	.443		.437
.72	.003	.009	.025	1.72	.458		.452
.74	.004	.010	.028	1.74	.474		.467
.76	.006	.012	.031	1.76	.491		.482
.78	.008	.013	.035	1.78	.507		.497
.80	.011	.014	.038	1.80	.524		.512
.82	.014	.016	.041	1.82	.541		.532
.84	.017	.017	.045	1.84	.558		.551
.86	.020	.019	.049	1.86	.576		.570
.88	.023	.021	.054	1.88	.594		.589
.90	.027	.024	.059	1.90	.611		.607
.92	.031	.026	.064	1.92	.630		.628
.94	.036	.028	.067	1.94	.648		.648
.96	.040	.030	.075	1.96	.667		.667
.98	.045	.033	.081	1.98	.686		.686
1.00	.050	.036	.086	2.00	.705		.706
1.02	.056	.039	.092	2.02	.725		.726
1.04	.062	.043	.098	2.04	.744		.746
1.06	.069	.046	.106	2.06	.764		.766
1.08	.076	.051	.112	2.08	.784		.786
1.10	.084	.055	.120	2.10	.805		.806
1.12	.092	.059	.127	2.12	.826		.827
1.14	.101	.064	.134	2.14	.846		.847
1.16	.110	.068	.141	2.16	.867		.868
1.18	.119	.073	.150	2.18	.889		.888
1.20	.128	.078	.158	2.20	.910		.910
1.22	.138	.084	.166	2.22			.931
1.24	.148	.089	.174	2.24			.953
1.26	.158	.095	.182	2.26			.975
1.28	.168	.101	.191	2.28			.998
1.30	.179	.107	.200	2.30			1.020
1.32	.190	.113	.209	2.32			1.045
1.34	.201	.120	.218	2.34			1.068
1.36	.212	.127	.227	2.36			1.091
1.38	.223	.135	.238	2.38			1.114
1.40	.236	.148	.250	2.40			1.138
1.42	.248	.151	.260	2.42			1.162
1.44	.260	.160	.270	2.44			1.187
1.46	.273	.170	.281	2.46			1.214
1.48	.285	.179	.292	2.48			1.242

O: Oslo Correction

GF: Gold Foil Correction

TABLE 3. Intensity of Scattered Electrons Striking Photographic Plate (I_p).

	48 cm	370°K	19 cm	370°K	GF	473°K
s	Oslo	GF	Oslo	GF	48 cm	19 cm
1.50	4.6019	4.6105				
1.75	4.8090	4.8232				
2.00	5.7383	5.7660			6.3855	
2.25	6.5394	6.5461			7.2846	
2.50	6.9290	6.9147			7.7183	
2.75	7.0799	7.0592			7.8778	
3.00	7.3298	7.2938			8.1309	
3.25	7.8104	7.7402			8.6209	
3.50	8.2010	8.0925			9.0426	
3.75	8.3439	8.2308			9.0559	
4.00	7.7902	7.7208			8.4042	
4.25	6.8496	6.8412			7.3737	
4.50	5.9291	5.9532			6.5944	
4.75	5.5201	5.5491			6.1090	
5.00	5.7169	5.7451			6.3410	
5.25	6.3675	6.3800			7.0105	
5.50	7.1157	7.0886			7.7184	
5.75	7.5679	7.5134			8.1458	
6.00	7.5754	7.5206			8.1055	
6.25	7.2573	7.2235			7.7592	
6.50	6.8933	6.8793			7.3755	
6.75	6.6716	6.6707			7.2321	
7.00	6.6643	6.6637	10.1271	9.7884	7.2920	27.9400
7.25	6.7914	6.7820	9.9084	9.6000	7.1433	27.5335
7.50	6.9340	6.9180	9.7374	9.4505	7.2553	27.3350
7.75	7.0380	7.0166	9.5300	9.2685	7.3726	27.1162
8.00	7.1536	7.1237	9.3493	9.1008	7.5203	26.9412
8.25	7.3564	7.3150	9.3266	9.0805	7.7161	26.8706
8.50	7.6226	7.5628	9.4040	9.1547	7.9617	26.8930
8.75	7.9055	7.8247	9.4521	9.2009	8.1837	26.8463
9.00	8.0610	7.9674	9.3239	9.0870	8.2773	26.6129
9.25	8.0121	7.9218	8.9530	8.7573	8.1675	23.0653
9.50	7.7555	7.6825	8.3375	8.2099	8.0106	24.7685
9.75	7.4433	7.3942	7.7580	7.6865	7.5876	23.5161
10.00	7.2452	7.2096	7.3222	7.2860	7.3955	22.6222
10.25	7.2815	7.2432	7.2006	7.1719	7.4371	22.2296
10.50	7.5390	7.4804	7.2924	7.2594	7.6518	22.3070
10.75	7.8860	7.8041	7.4349	7.3909	7.9413	22.6103
11.00	8.1750	8.0644	7.5142	7.4620	8.1616	22.6775
11.25	8.2947	8.1794	7.4393	7.3945	8.2505	22.6105
11.50	8.2561	8.1435	7.2130	7.1821	8.1847	22.2181
11.75	8.0323	8.0054	6.9010	6.8928	8.0332	21.5200

Oslo, GF Indicates Blackness Correction Applied.

TABLE 3. Continued.

	48 cm	370°K	19 cm	370°K	GF	473°K
s	Oslo	GF	Oslo	GF	48 cm	19 cm
12.00	7.9568	7.8673	6.6461	6.6522	7.8556	20.8913
12.25	7.8495	7.7662	6.4492	6.4657	7.6911	20.3446
12.50	7.7851	7.7050	6.2958	6.3176	7.5922	19.9227
12.75	7.7611	7.6813	6.1875	6.2115	7.5282	19.6179
13.00	7.7686	7.6885	6.1006	6.1261	7.5094	19.4176
13.25	7.8128	7.7247	6.0554	6.0816	7.5398	19.3429
13.50	7.8990	7.8096	6.0542	6.0804	7.6128	19.3369
13.75	8.0307	7.9314	6.0730	6.0989	7.7209	19.3986
14.00	8.1514	8.0444	6.0971	6.1226	7.7813	19.4307
14.25	8.1978	8.0863	6.0671	6.0927	7.7766	19.2778
14.50	8.1653	8.0561	5.9596	5.9855	7.6763	18.9771
14.75	8.0276	7.9283	5.7852	5.8107	7.5174	18.7458
15.00	7.8653	7.7730	5.5886	5.6118	7.3642	17.9845
15.25	7.7386	7.6544	5.4413	5.4611	7.2233	17.4931
15.50	7.6779	7.6341	5.3535	5.3719	7.1486	17.3098
15.75	7.7311	7.6479	5.3400	5.3582	7.1578	17.2813
16.00	7.8441	7.7482	5.3807	5.4004	7.2280	17.3066
16.25	7.9544	7.8581	5.4142	5.4322	7.2918	17.3483
16.50	8.0323	7.9395	5.4183	5.4366	7.3388	17.3354
16.75	8.0509	7.9461	5.3780	5.3974	7.3252	17.2387
17.00	8.0135	7.9114	5.3094	5.3267	7.2610	17.0546
17.25	7.9267	7.8286	5.2174	5.2360	7.1575	16.8068
17.50	7.8404	7.7421	5.1255	5.1432	7.0397	16.5123
17.75	7.7438	7.6606	5.0521	5.0693	6.9401	16.2431
18.00	7.6878	7.6078	4.9814	4.9979	6.8618	16.0742
18.25	7.6668	7.5891	4.9338	4.9499	6.8085	15.9308
18.50	7.6628	7.5852	4.9124	4.9283	6.7892	15.8883
18.75	7.7089	7.6264	4.9217	4.9376	6.8043	15.8893
19.00	7.7564	7.6646	4.9420	4.9583	6.8337	15.9169
19.25	7.7990	7.7046	4.9645	4.9811	6.8564	15.9086
19.50			4.9603	4.9769	6.8472	15.8424
19.75			4.9246	4.9408	6.8177	15.7339
20.00			4.8590	4.8748	6.7875	15.5388
20.25			4.7806	4.7957		15.3040
20.50			4.7065	4.7209		15.1021
20.75			4.6537	4.6675		14.9834
21.00			4.6314	4.6448		14.8901
21.25			4.6334	4.6468		14.8761
21.50			4.6506	4.6644		14.8591
21.75			4.6637	4.6775		14.8485
22.00			4.6658	4.6797		14.8240
22.25			4.6458	4.6593		14.7386
22.50			4.6031	4.6161		14.6058
22.75			4.5526	4.5649		14.4778

TABLE 3. Continued.

	48 cm	370°K	19 cm	370°K	GF	473°K
s	Oslo	GF	Oslo	GF	48 cm	19 cm
23.00			4.5021	4.5138		14.3094
23.25			4.4496	4.4602		14.1560
23.50			4.4163	4.4263		14.0466
23.75			4.4013	4.4109		13.9783
24.00			4.4013	4.4110		13.9478
24.25			4.4063	4.4160		13.9173
24.50			4.4124	4.4222		13.9008
24.75			4.4114	4.4211		13.8648
25.00			4.3962	4.4057		13.7892
25.25			4.3649	4.3738		13.6823
25.50			4.3257	4.3339		13.5537
25.75			4.2815	4.2889		13.4006
26.00			4.2424	4.2491		13.2927
26.25			4.2163	4.2225		13.1928
26.50			4.2063	4.2123		13.1287
26.75			4.2022	4.2082		13.0851
27.00			4.2062	4.2122		13.0653
27.25			4.2091	4.2152		13.0312
27.50			4.2021	4.2081		12.9889
27.75			4.1882	4.1941		12.9130
28.00			4.1639	4.1697		12.8283
28.25			4.1300	4.1353		12.7278
28.50			4.1050	4.1099		12.6102
28.75			4.0770	4.0815		12.5339
29.00			4.0579	4.0622		12.4542
29.25			4.0448	4.0489		12.3933
29.50			4.0398	4.0438		12.3613
29.75			4.0378	4.0417		12.3247
30.00			4.0358	4.0396		12.2879
30.25			4.0287	4.0325		12.2394
30.50			4.0167	4.0202		12.1721
30.75			3.9976	4.0009		12.1080
31.00			3.9718	3.9748		12.0271
31.25			3.9487	3.9516		11.9358
31.50			3.9257	3.9285		11.8750
31.75			3.9097	3.9123		11.8144
32.00			3.9007	3.9032		11.7642
32.25			3.8987	3.9012		11.7114
32.50			3.8956	3.8981		11.6765
32.75			3.8896	3.8920		11.6468
33.00			3.8796	3.8820		11.5919
33.25			3.8686	3.8709		11.5428
33.50			3.8586	3.8608		11.4863
33.75			3.8445	3.8466		11.4226

TABLE 3. Continued.

	48 cm	370°K	19 cm	370°K	GF	473°K
s	Oslo	GF	Oslo	GF	48 cm	19 cm
34.00			3.8285	3.8306		11.3528
34.25			3.8126	3.8146		11.2949
34.50			3.8005	3.8025		11.2339
34.75			3.7945	3.7964		11.1820
35.00			3.7886	3.7904		11.1478
35.25			3.7825	3.7843		11.1129
35.50			3.7745	3.7762		11.0780
35.75			3.7695	3.7712		11.0361
36.00			3.7605	3.7621		10.9820
36.25			3.7506	3.7522		10.9127
36.50			3.7336	3.7350		10.8528
36.75			3.7186	3.7200		10.7958
37.00			3.7024	3.7038		10.7469
37.25			3.6965	3.6978		10.7005
37.50			3.6925	3.6938		10.6562
37.75			3.6895	3.6908		10.6175
38.00			3.6885	3.6898		10.5735
38.25			3.6836	3.6849		10.5297
38.50			3.6785	3.6798		10.4847
38.75			3.6685	3.6698		10.4408
39.00			3.6594	3.6606		10.3939
39.25			3.6495	3.6506		10.3452
39.50			3.6385	3.6396		10.3041
39.75			3.6315	3.6326		10.2571
40.00			3.6255	3.6266		10.2051
40.25						10.1690
40.50						10.1337
40.75						10.1050
41.00						10.0486
41.25						10.0137
41.50						9.9718
41.75						9.9372
42.00						9.8953
42.25						9.8540
42.50						9.8148
42.75						9.7697
43.00						9.7260
43.25						9.6883
43.50						9.6504
43.75						9.6181
44.00						9.5845
44.25						9.5391
44.50						9.5004
44.75						9.4598
45.00						9.4268

After the densities were corrected, corresponding points on each branch and each trace for a given camera distance and temperature were averaged to give a composite curve, I_p.

The intensity per unit solid angle, I_t, is related to I_p by the equation

$$I_p(s) = I_t(s) \cdot \alpha(r_s) \cdot \cos^3 \Theta \qquad (18)$$

The sector, which rotates in a plane parallel to and slightly above the photographic plate, modifies I_t in a way which is a function of the sector shape. The sector shape is given by $\alpha(r_s) = \rho r^3$. ρ is approximately constant except for small s, r is the radius on the sector measured from the undiffracted beam position, and α is the angular opening. The factor $\cos^3 \Theta$ takes account of the fact that the photographic plate is perpendicular to the undiffracted beam and thus not everywhere equidistant from the scattering point (Figure 5): the inverse square drop-off of intensity with distance leads to $\cos^2 \Theta$ and the inclination of the plate at angle Θ to the diffracted rays leads additionally to $\cos \Theta$.

The total intensity may be represented by the equation

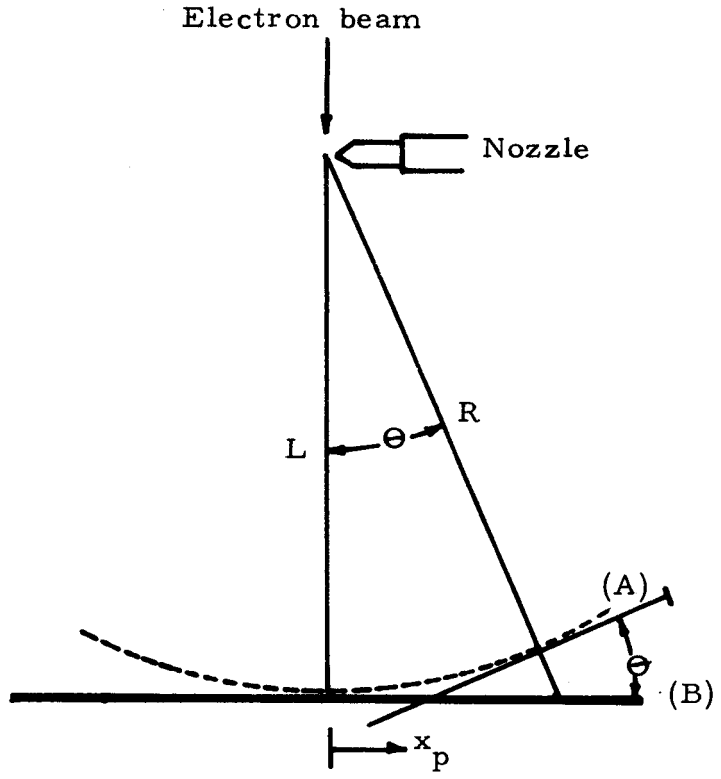

FIGURE 5. Relation of Plate Position to Plate Exposure.

(A) Position of a Theoretical Photographic Plate.
(B) Actual Position of Plates.

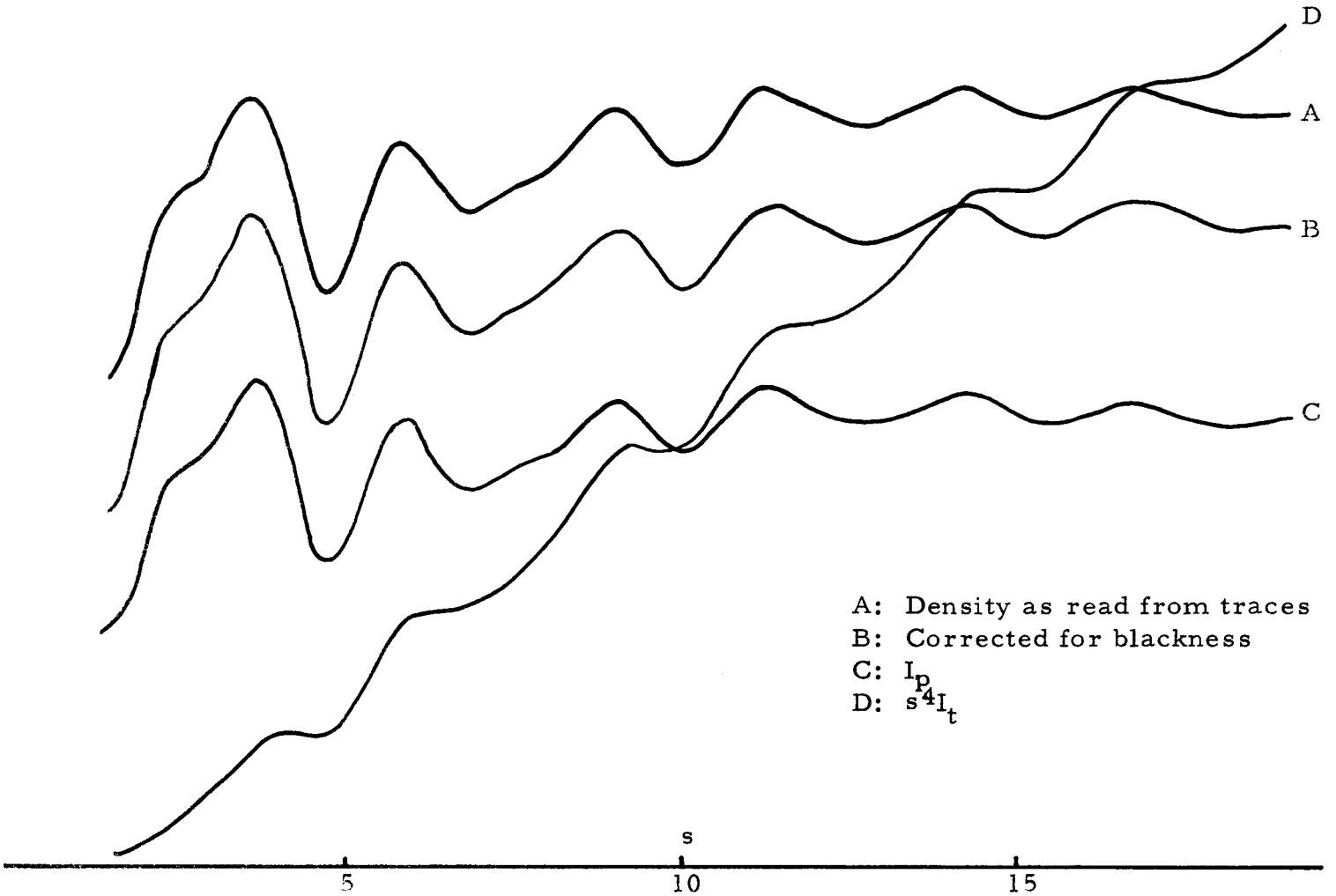

FIGURE 6. Various kinds of Intensity Curves.

$$I_t(s) = k \sum_{i,j}{}' \frac{(Z-f)_i (Z-f)_j}{s^5 r_{ij}} e^{\frac{-l_{ij}^2 s^2}{2}} \sin sr_{ij}$$

$$+ k \sum_i \frac{(Z-f)_i^2}{s^4} + k \sum_i \frac{S_i}{s^4} + B_{ext.} \qquad (19)$$

where the summations extend over all atoms i and j in the molecule. The term $B_{ext.}$ is due to extraneous scattering from the diffraction apparatus. Z_i represents the atomic number of the i^{th} atom, r_{ij} the internuclear separation of the i^{th} and j^{th} atom, l_{ij} the root-mean-square amplitude of vibration of the atom pair associated with the distance r_{ij}, f_i is the x-ray form factor, and S_i is the incoherent scattering factor.

Since only the first summation is sensitive to molecular structure, this part, $\frac{I_m}{s^4}$, is next separated from the remaining "background" intensity. This is possible because of the smooth functional dependence of the second and third terms of equation (19). By plotting the experimental total intensity on large-size graph paper (Figure 7) a smooth curve representing the background may be drawn through the undulations deriving from the first term of equation (19) and subtracted from the total intensity (6, p. 815-821). Since the total intensities obtained from electron diffraction experiments decrease very rapidly with increasing s, it is convenient to first multiply them by s^4 to deaccentuate this decline before subtracting the background.

TABLE 4. The Function $s^4/\alpha(r_s) \cdot \cos^3(\Theta)$.

	370°K		473°K			370°K		473°K	
s	48 cm	19 cm	48 cm	19 cm	s	48 cm	19 cm	48 cm	19 cm
.00	0.00		0.00		10.00	344.86	45.57	337.92	43.82
.25	0.01		0.01		10.25	353.60	47.91	346.55	46.07
.50	0.12		0.12		10.50	362.41	50.39	355.19	48.32
.75	0.64		0.64		10.75	371.25	52.73	363.85	50.57
1.00	2.17		2.18		11.00	380.11	55.18	372.54	52.87
1.25	5.44		5.43		11.25	388.98	57.66	381.23	55.14
1.50	10.83		10.79		11.50	397.84	60.09	389.90	57.37
1.75	17.92		17.79		11.75	406.68	62.44	398.56	59.54
2.00	25.81		25.55		12.00	415.50	64.73	407.20	61.65
2.25	33.32		32.88		12.25	424.32	66.96	415.83	63.72
2.50	41.18		40.63		12.50	433.11	69.16	424.45	65.75
2.75	49.68		49.00		12.75	441.91	71.33	433.06	67.76
3.00	59.08		58.29		13.00	450.67	73.47	441.62	69.73
3.25	69.31		68.38		13.25	459.39	75.58	450.15	71.64
3.50	80.16		79.06		13.50	468.08	77.66	458.66	73.57
3.75	91.85		90.61		13.75	476.76	79.72	467.16	75.50
4.00	104.73		103.31		14.00	485.44	81.74	475.67	77.43
4.25	117.79		116.13		14.25	494.11	83.77	484.16	79.36
4.50	130.73		128.74		14.50	502.78	85.78	492.65	81.29
4.75	142.90		140.57		14.75	511.44	87.82	501.13	83.22
5.00	154.50	10.88	151.88	10.58	15.00	520.09	89.90	509.60	85.15
5.25	165.57	12.36	162.68	11.95	15.25	528.73	91.98	518.06	87.16
5.50	176.59	13.80	173.49	13.26	15.50	537.37	94.08	526.53	89.14
5.75	187.61	15.12	184.29	14.51	15.75	546.03	96.17	535.02	91.04
6.00	198.86	16.48	195.33	15.81	16.00	554.72	98.24	543.55	92.92
6.25	209.73	17.89	205.86	17.16	16.25	563.46	100.28	552.13	94.73
6.50	219.85	19.36	215.68	18.57	16.50	572.23	102.25	560.73	96.50
6.75	229.46	20.84	224.99	19.99	16.75	581.04	104.17	569.38	98.24
7.00	238.65	22.38	233.97	21.48	17.00	589.88	106.03	578.05	99.94
7.25	247.73	24.00	242.85	23.04	17.25	598.74	107.84	586.73	101.61
7.50	256.70	25.69	251.62	24.66	17.50	607.61	109.62	595.41	103.24
7.75	265.54	27.44	260.26	26.33	17.75	616.45	111.37	604.06	104.86
8.00	274.34	29.23	268.88	28.06	18.00	625.28	113.11	612.68	106.48
8.25	283.12	31.08	277.49	29.85	18.25	634.02	114.82	621.14	108.09
8.50	291.94	33.02	286.14	31.68	18.50	642.60	116.54	629.58	109.69
8.75	300.77	34.99	294.79	33.55	18.75	651.25	118.25	638.08	111.29
9.00	309.60	37.00	303.44	35.45	19.00	659.98	119.96	646.70	112.88
9.25	318.42	39.05	312.07	37.42	19.25	668.85	121.66	655.41	114.47
9.50	327.21	41.15	320.68	39.45	19.50	677.77	123.35	664.19	116.04
9.75	336.00	43.32	329.30	41.57	19.75	686.75	125.03	673.00	117.62

TABLE 4. Continued.

	370°K		473°K			370°K		473°K	
s	48 cm	19 cm	48 cm	19 cm	s	48 cm	19 cm	48 cm	19 cm
20.00		126.71		119.19	30.00		195.33		183.67
20.25		128.39		120.76	30.25		197.09		185.32
20.50		130.06		122.33	30.50		198.86		186.98
20.75		131.73		123.90	30.75		200.62		188.64
21.00		133.41		125.47	31.00		202.39		190.30
21.25		135.08		127.05	31.25		204.16		191.96
21.50		136.76		128.64	31.50		205.93		193.62
21.75		138.45		130.23	31.75		207.71		195.29
22.00		140.14		131.82	32.00		209.48		196.95
22.25		141.83		133.41	32.25		211.26		198.62
22.50		143.52		135.00	32.50		213.04		200.28
22.75		145.22		136.60	32.75		214.82		201.94
23.00		146.92		138.19	33.00		216.60		203.60
23.25		148.62		139.79	33.25		218.38		205.26
23.50		150.32		141.38	33.50		220.15		206.92
23.75		152.02		142.97	33.75		221.93		208.59
24.00		153.72		144.57	34.00		223.70		210.26
24.25		155.42		146.17	34.25		225.48		211.93
24.50		157.13		147.77	34.50		227.27		213.60
24.75		158.83		149.37	34.75		229.05		215.28
25.00		160.54		150.97	35.00		230.84		216.96
25.25		162.24		152.58	35.25		232.68		218.64
25.50		163.96		154.19	35.50		234.42		220.32
25.75		165.67		155.80	35.75		236.22		222.00
26.00		167.39		157.42	36.00		238.02		223.69
26.25		169.11		159.04	36.25		239.82		225.38
26.50		170.84		160.66	36.50		241.62		227.07
26.75		172.56		162.29	36.75		243.42		228.26
27.00		174.29		163.91	37.00		245.23		230.46
27.25		176.03		165.55	37.25		247.05		232.16
27.50		177.77		167.19	37.50		248.86		233.86
27.75		179.51		168.83	37.75		250.67		235.56
28.00		181.25		170.47	38.00		252.49		237.27
28.25		183.01		172.12	38.25		254.31		238.98
28.50		184.76		173.77	38.50		256.14		240.69
28.75		186.52		175.41	38.75		257.96		242.42
29.00		188.28		177.06	39.00		259.80		244.15
29.25		190.04		178.71	39.25		261.64		245.88
29.50		191.80		180.36	39.50		263.48		247.63
29.75		193.56		182.02	39.75		265.33		249.38

TABLE 5. Intensity per unit Solid Angle, $I_t(s)$ (x s^4).

	48 cm	370°K	19 cm	370°K	GF	473°K
s	$(I_t)_O$	$(I_t)_{GF}$	$(I_t)_O$	$(I_t)_{GF}$	$(I_t)_{48}$	$(I_t)_{19}$
1.50	49	49				
1.75	86	86				
2.00	148	148			163	
2.25	217	218			239	
2.50	285	284			313	
2.75	351	350			386	
3.00	433	430			473	
3.25	541	536			589	
3.50	657	648			714	
3.75	766	756			820	
4.00	815	808			868	
4.25	806	805			856	
4.50	775	778			848	
4.75	788	792			858	
5.00	883	887			963	
5.25	1054	1056			1140	
5.50	1256	1251			1339	
5.75	1419	1409			1501	
6.00	1506	1495			1583	
6.25	1522	1514			1597	
6.50	1515	1512			1590	
6.75	1530	1530			1627	
7.00	1590	1590	2266	2190	1706	6002
7.25	1682	1680	2378	2304	1734	6343
7.50	1779	1775	2501	2428	1825	6739
7.75	1868	1863	2614	2542	1918	7139
8.00	1962	1954	2732	2659	2022	7559
8.25	2082	2071	2899	2822	2141	8020
8.50	2232	2215	3104	3022	2278	8520
8.75	2377	2353	3307	3219	2412	9006
9.00	2495	2466	3449	3361	2511	9433
9.25	2551	2522	3496	3420	2548	8630
9.50	2537	2513	3431	3378	2568	9771
9.75	2500	2484	3360	3329	2498	9775
10.00	2498	2485	3337	3320	2499	9912
10.25	2574	2561	3450	3436	2577	10240
10.50	2732	2710	3667	3651	2717	10778
10.75	2927	2897	3920	3897	2889	11434
11.00	3107	3065	4146	4117	3040	11990
11.25	3226	3181	4289	4264	3145	12468
11.50	3284	3239	4334	4315	3191	12745
11.75	3300	3355	4308	4303	3201	12813

O, GF Indicates Blackness Correction Applied

TABLE 5. Continued.

	48 cm	370°K	19 cm	370°K	GF	473°K
s	$(I_t)_O$	$(I_t)_{GF}$	$(I_t)_O$	$(I_t)_{GF}$	$(I_t)_{48}$	$(I_t)_{19}$
12.00	3306	3268	4302	4305	3198	12879
12.25	3330	3295	4318	4329	3198	12962
12.50	3371	3337	4354	4369	3222	13099
12.75	3429	3394	4413	4430	3260	13293
13.00	3501	3464	4482	4500	3316	13539
13.25	3589	3548	4576	4596	3394	13858
13.50	3697	3655	4701	4722	3491	14226
13.75	3828	3781	4841	4861	3606	14645
14.00	3957	3905	4983	5004	3701	15045
14.25	4050	3995	5082	5103	3765	15298
14.50	4105	4050	5112	5134	3781	15425
14.75	4105	4054	5080	5103	3767	15600
15.00	4090	4042	5023	5044	3752	15314
15.25	4091	4047	5004	5023	3742	15247
15.50	4125	4084	5036	5054	3763	15429
15.75	4221	4175	5135	5153	3829	15735
16.00	4351	4298	5286	5305	3928	16081
16.25	4482	4427	5429	5447	4026	16434
16.50	4596	4537	5540	5558	4115	16729
16.75	4677	4616	5602	5622	4170	16935
17.00	4726	4666	5629	5647	4197	17045
17.25	4746	4687	5626	5646	4199	17076
17.50	4763	4704	5618	5637	4191	17046
17.75	4773	4722	5626	5645	4192	17032
18.00	4807	4757	5634	5653	4204	17115
18.25	4860	4811	5665	5683	4229	17219
18.50	4924	4874	5724	5743	4274	17428
18.75	5020	4966	5820	5838	4341	17683
19.00	5119	5058	5928	5948	4419	17967
19.25	5216	5153	6039	6059	4493	18210
19.50			6118	6138	4547	18383
19.75			6157	6177	4588	18505
20.00			6157	6177	4628	18520
20.25			6137	6157		18481
20.50			6121	6140		18474
20.75			6130	6148		18564
21.00			6178	6196		18683
21.25			6258	6277		18900
21.50			6360	6379		19114
21.75			6456	6475		19336
22.00			6538	6557		19540
22.25			6589	6608		19662
22.50			6606	6625		19717
22.75			6611	6629		19776

TABLE 5. Continued.

	48 cm	370°K	19 cm	370°K	GF	473°K
s	$(I_t)_O$	$(I_t)_{GF}$	$(I_t)_O$	$(I_t)_{GF}$	$(I_t)_{48}$	$(I_t)_{19}$
23.00			6614	6631		19774
23.25			6612	6628		19787
23.50			6638	6653		19858
23.75			6690	6705		19985
24.00			6765	6780		20164
24.25			6848	6863		20342
24.50			6933	6948		20540
24.75			7006	7022		20709
25.00			7057	7072		20818
25.25			7081	7096		20876
25.50			7092	7105		20898
25.75			7093	7105		20878
26.00			7101	7112		20925
26.25			7130	7140		20981
26.50			7185	7196		21092
26.75			7251	7261		21235
27.00			7331	7341		21415
27.25			7409	7419		21572
27.50			7469	7480		21715
27.75			7518	7528		21801
28.00			7547	7557		21869
28.25			7558	7567		21907
28.50			7584	7593		21912
28.75			7604	7613		21986
29.00			7636	7644		22051
29.25			7686	7694		22148
29.50			7748	7755		22295
29.75			7815	7823		22432
30.00			7883	7890		22569
30.25			7940	7947		22682
30.50			7987	7994		22759
30.75			8020	8026		22840
31.00			8038	8044		22887
31.25			8061	8067		22911
31.50			8084	8090		22992
31.75			8120	8126		23072
32.00			8171	8176		23170
32.25			8236	8241		23260
32.50			8299	8304		23385
32.75			8355	8361		23519
33.00			8403	8408		23600
33.25			8448	8453		23692
33.50			8494	8499		23767
33.75			8531	8536		23826

TABLE 5. Continued.

	48 cm	370°K	19 cm	370°K	GF	473°K
s	$(I_t)_O$	$(I_t)_{GF}$	$(I_t)_O$	$(I_t)_{GF}$	$(I_t)_{48}$	$(I_t)_{19}$
34.00			8564	8569		23870
34.25			8596	8601		23937
34.50			8637	8641		23995
34.75			8691	8695		24072
35.00			8745	8749		24185
35.25			8799	8803		24296
35.50			8848	8852		24406
35.75			8904	8908		24500
36.00			8950	8954		24565
36.25			8994	8998		24594
36.50			9021	9024		24643
36.75			9052	9055		24696
37.00			9079	9082		24767
37.25			9131	9135		24841
37.50			9189	9192		24920
37.75			9248	9251		25010
38.00			9313	9316		25087
38.25			9367	9371		25163
38.50			9422	9425		25235
38.75			9463	9466		25310
39.00			9506	9510		25376
39.25			9548	9551		25437
39.50			9586	9589		25515
39.75			9635	9638		25579
40.00			9687	9690		25628
40.25						25717
40.50						25807
40.75						25914
41.00						25949
41.25						26038
41.50						26108
41.75						26196
42.00						26265
42.25						26333
42.50						26406
42.75						26462
43.00						26520
43.25						26593
43.50						26664
43.75						26749
44.00						26828
44.25						26870
44.50						26931
44.75						26986
45.00						27062

The question may arise as to the contribution of the extraneous background to the experimental background. An estimate of its contribution may be gotten by computing the second and third terms of equation (19) and comparing this "theoretical" background to the total (30, p. 748-769). The calculation of this theoretical background presented some difficulties as accurate values of S were not available for arsenic or bromine, and were estimated by extrapolating the values available for copper and germanium (18, p. 274-281; 17, p. 929-932). In Figure 8 the experimental background and the theoretical background are shown. The deviation of the two backgrounds from one another is attributed to the extraneous background contribution, and inaccuracies in evaluating S_{As} and S_{Br}.

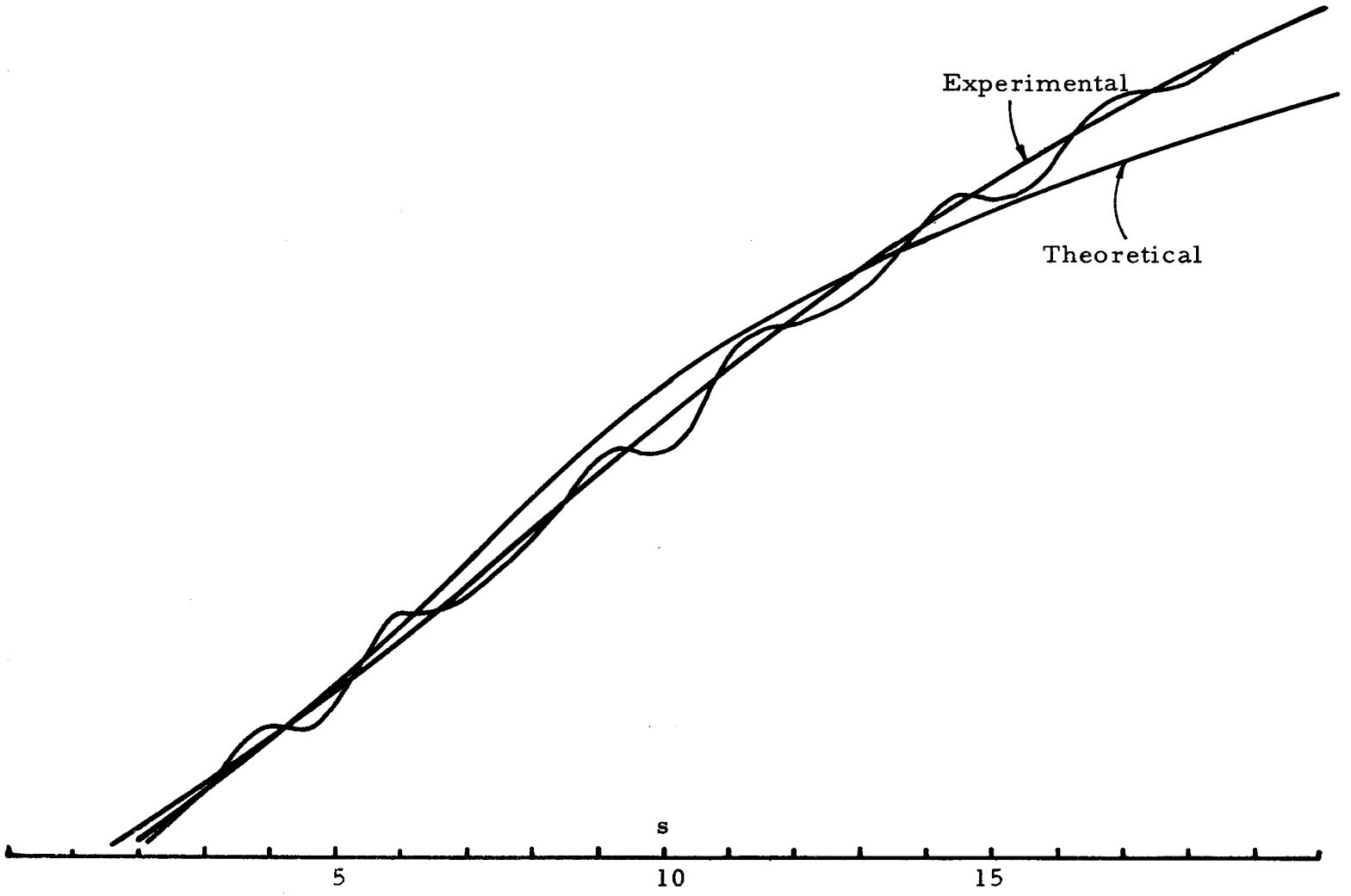

FIGURE 7. Experimental and Theoretical Backgrounds.

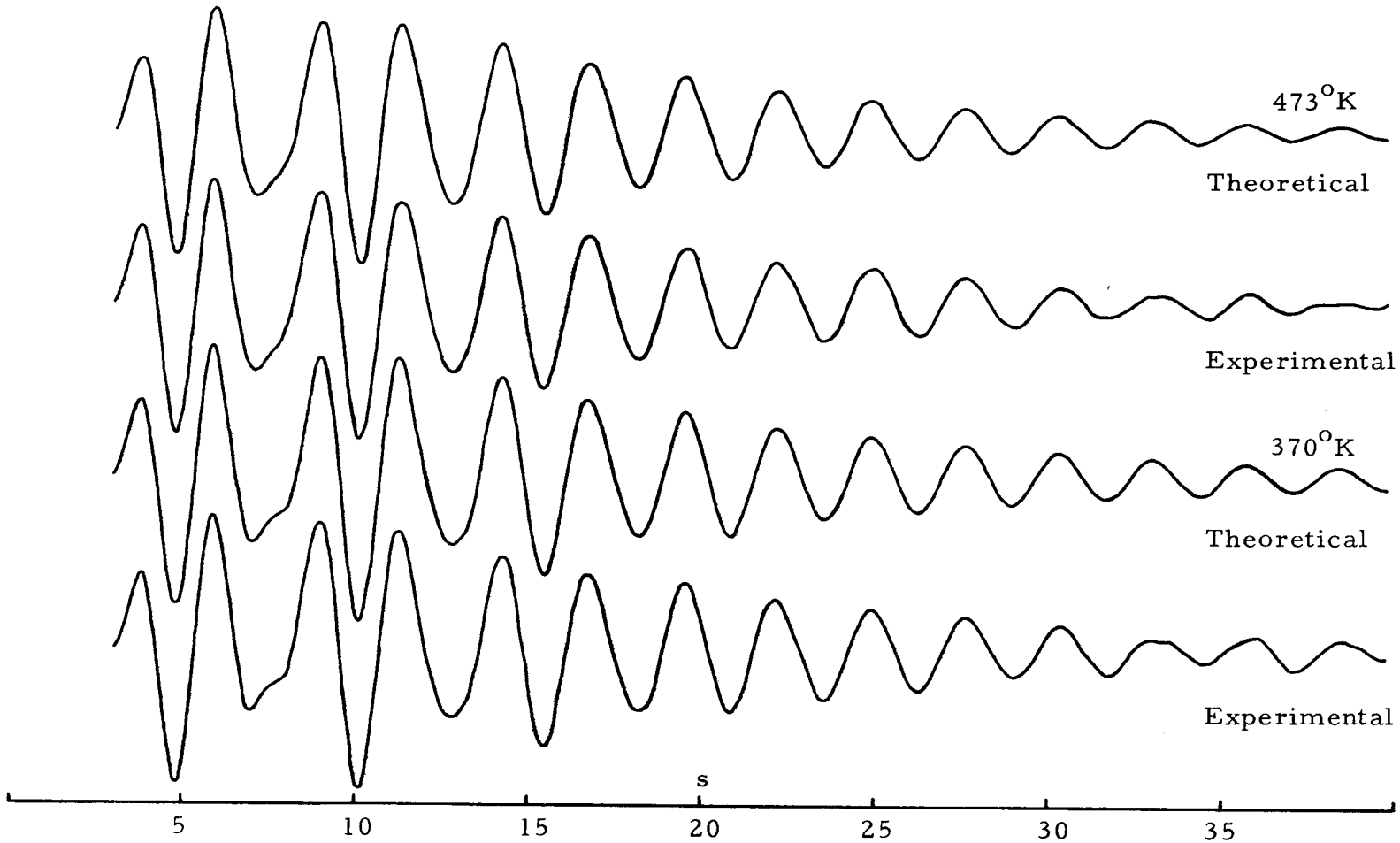

FIGURE 8. Experimental and Theoretical Molecular Intensity Curves, $I_m(s)$, for Arsenic Tribromide.

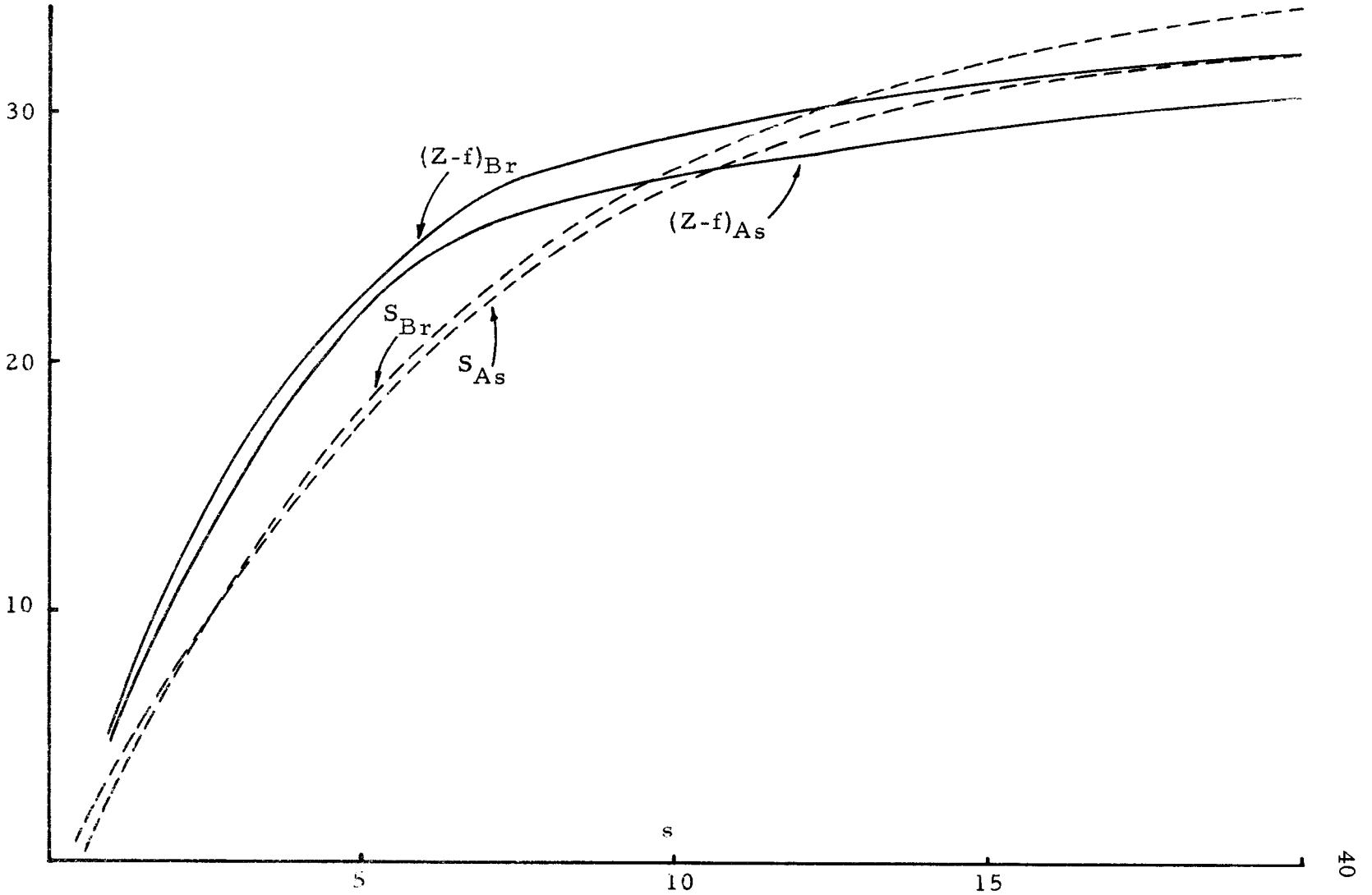

FIGURE 9. $(Z-f)_i$ and S_i curves for Arsenic and Bromine.

TABLE 6. Molecular Intensity Curves for Arsenic Tribromide.*

	370°K		473°K			370°K		473°K	
s	Exp.	Theo.	Exp.	Theo.	s	Exp.	Theo.	Exp.	Theo.
.00					10.00	-38.92	-40.23	-37.65	-36.77
.25					10.25	-38.89	-40.29	-36.13	-35.97
.50					10.50	-21.36	-22.68	-20.59	-20.15
.75					10.75	3.73	3.27	1.54	2.66
1.00					11.00	24.39	24.97	19.05	21.98
1.25					11.25	33.55	33.75	28.76	30.56
1.50					11.50	28.82	28.63	27.21	27.22
1.75					11.75	14.46	15.12	14.96	15.86
2.00					12.00	0.81	0.47	2.87	2.08
2.25					12.25	-9.94	-10.57	-9.56	-9.79
2.50					12.50	-16.94	-17.03	-16.87	-17.75
2.75					12.75	-19.70	-19.95	-20.20	-21.25
3.00	-1.17	0.07	0.52	0.35	13.00	-19.43	-19.66	-19.24	-19.86
3.25	4.90	6.68	7.34	6.95	13.25	-15.28	-15.07	-13.31	-13.25
3.50	13.06	16.30	15.98	16.26	13.50	-6.12	-5.13	-3.19	-2.03
3.75	21.22	21.68	22.33	21.15	13.75	7.20	8.83	10.16	11.17
4.00	15.86	15.61	15.98	14.79	14.00	20.81	22.11	20.93	21.76
4.25	-1.63	-2.34	-3.28	-2.92	14.25	26.82	28.57	24.74	25.24
4.50	-24.25	-24.07	-25.84	-23.87	14.50	23.23	24.07	19.30	19.43
4.75	-38.24	-36.95	-37.44	-35.91	14.75	8.53	9.47	4.07	6.16
5.00	-32.88	-32.01	-30.25	-30.69	15.00	-10.21	-9.29	-9.16	-9.39
5.25	-10.73	-10.59	-10.29	-9.88	15.25	-23.46	-24.14	-22.31	-21.05
5.50	17.02	16.25	16.06	15.80	15.50	-28.24	-28.87	-24.39	-24.42
5.75	35.21	34.42	33.50	33.08	15.75	-21.88	-22.27	-17.40	-18.80
6.00	36.61	35.20	33.73	33.91	16.00	-6.98	-8.10	-5.59	-7.18
6.25	22.38	20.97	19.27	20.65	16.25	8.26	7.25	6.69	5.81
6.50	3.26	1.07	0.09	1.89	16.50	18.17	18.10	14.74	15.58
6.75	-12.12	-13.83	-14.24	-12.65	16.75	21.40	21.64	19.44	19.46
7.00	-17.72	-19.10	-19.27	-18.66	17.00	18.14	18.19	16.70	17.00
7.25	-15.16	-17.36	-19.27	-18.14	17.25	8.97	10.13	9.65	9.70
7.50	-12.12	-14.04	-15.32	-15.40	17.50	-1.02	0.28	-1.06	0.09
7.75	-10.03	-12.06	-12.49	-12.66	17.75	-9.61	-8.90	-9.85	-9.02
8.00	-7.63	-9.47	-4.37	-8.38	18.00	-15.83	-15.42	-14.36	-15.09
8.25	0.87	-1.95	2.85	0.45	18.25	-17.64	-17.75	-16.35	-16.45
8.50	15.78	11.87	15.33	13.91	18.50	-16.36	-14.96	-12.80	-12.68
8.75	30.00	26.94	26.95	26.86	18.75	-8.51	-7.35	-5.36	-4.91
9.00	36.05	34.20	31.52	31.52	19.00	4.94	3.06	4.02	4.39
9.25	29.00	26.46	22.56	22.59	19.25	13.39	12.80	11.73	12.12
9.50	5.88	4.46	1.75	1.86	19.50	18.69	18.37	15.26	15.65
9.75	-20.30	-22.23	-21.68	-21.72	19.75	17.53	16.75	15.01	13.31

*These curves are composite curves formed by joining the 19cm and 48cm curves.

TABLE 6. Continued.

	370°K		473°K			370°K		473°K	
s	Exp.	Theo.	Exp.	Theo.	s	Exp.	Theo.	Exp.	Theo.
20.00	9.59	10.19	8.37	7.37	30.00	4.63	5.09	3.10	3.86
20.25	-1.32	-0.47	-1.25	-1.29	30.25	6.78	7.09	4.82	5.00
20.50	-11.74	-10.54	-10.01	-9.09	30.50	7.28	6.09	4.07	4.47
20.75	-17.69	-16.39	-12.51	-13.45	30.75	5.13	4.13	3.63	2.53
21.00	-17.20	-16.23	-12.51	-13.11	31.00	1.16	0.36	1.06	-0.13
21.25	-11.24	-10.65	-6.26	-8.52	31.25	-2.32	-3.35	-2.94	-2.58
21.50	-1.82	-2.04	0.00	-1.46	31.50	-5.79	-5.80	-3.32	-4.07
21.75	6.78	6.51	6.26	5.62	31.75	-6.95	-6.26	-3.69	-4.16
22.00	13.39	12.34	11.26	10.48	32.00	-5.79	-4.69	-2.82	-2.91
22.25	13.89	13.95	11.89	11.73	32.25	-2.65	-1.68	-0.81	-0.80
22.50	9.43	11.23	8.76	9.21	32.50	0.83	1.73	-0.31	1.45
22.75	2.98	5.26	5.00	3.90	32.75	2.65	4.41	2.69	3.10
23.00	-3.97	-2.06	-2.50	-2.39	33.00	3.31	5.56	2.44	3.65
23.25	-11.24	-8.52	-8.13	-7.63	33.25	2.98	4.87	2.75	3.00
23.50	-14.55	-12.17	-10.64	-10.20	33.50	3.31	2.63	2.50	1.47
23.75	-13.06	-11.91	-9.38	-9.38	33.75	1.49	-0.35	0.94	-0.51
24.00	-7.94	-7.81	-5.63	-5.57	34.00	-0.50	-3.07	-1.38	-2.17
24.25	-1.65	-1.22	0.00	-0.13	34.25	-2.98	-4.68	-2.19	-3.04
24.50	5.29	5.65	6.88	5.12	34.50	-3.81	-4.70	-3.50	-2.87
24.75	10.47	10.48	9.38	8.46	34.75	-2.48	-3.21	-3.75	-1.79
25.00	11.58	11.07	10.01	8.89	35.00	0.00	-0.75	-1.44	-0.21
25.25	8.43	8.92	8.13	6.41	35.25	1.32	1.83	0.38	1.35
25.50	3.31	3.31	3.13	1.97	35.50	2.32	3.69	2.44	2.38
25.75	-3.80	-3.14	-3.75	-2.87	35.75	3.64	4.27	3.50	2.58
26.00	-9.59	-8.24	-6.88	-6.53	36.00	4.13	3.45	3.07	1.94
26.25	-11.74	-10.38	-9.38	-7.88	36.25	3.64	1.56	0.56	0.72
26.50	-9.92	-9.03	-8.13	-6.61	36.50	0.00	-0.74	-0.94	-0.66
26.75	-6.12	-4.85	-4.38	-3.29	36.75	-2.48	-2.69	-1.94	-1.73
27.00	0.00	0.65	0.00	0.92	37.00	-5.79	-3.67	-1.94	-2.18
27.25	5.79	5.67	4.38	4.60	37.25	-4.80	-3.42	-1.50	-1.90
27.50	8.76	8.63	7.51	6.60	37.50	-3.31	-2.09	-0.94	-1.03
27.75	9.26	8.71	6.88	6.39	37.75	-1.32	-0.15	0.19	0.11
28.00	6.95	6.03	5.63	4.13	38.00	1.32	1.74	0.25	1.15
28.25	1.48	1.53	2.50	0.65	38.25	2.48	2.97	0.56	1.75
28.50	-1.65	-3.28	-3.13	-2.85	38.50	3.47	3.18	0.69	1.75
28.75	-5.46	-6.85	-5.00	-5.24	38.75	2.31	2.36	0.62	1.19
29.00	-7.61	-8.09	-6.26	-5.82	39.00	1.65	0.82	0.13	0.28
29.25	-6.61	-6.66	-6.26	-4.49	39.25	0.00	-0.90	-0.50	-0.65
29.50	-3.47	-3.13	-2.50	-1.79	39.50	-1.65	-2.24	-0.06	-1.31
29.75	0.00	1.28	0.00	1.34	39.75	-1.32	-2.79	0.56	-1.51

DETERMINATION OF MOLECULAR STRUCTURE

The problem of the determination of gas phase molecular structures by electron diffraction consists in analyzing the molecular intensity curves for the precise values of the internuclear distances and the root-mean-square amplitudes of vibration that give rise to the curves. This may be done in simple cases such as arsenic tribromide by computing the scattered intensity to be expected theoretically from models of the molecule and comparing these theoretical intensity curves to the experimental curve; the "best" model is the one giving the closest agreement between the theoretical and observed curves. However, the availability of high speed computers with their capacity to handle large amounts of data has made possible an improved method of intensity "curve fitting" based on least-squares (5, p. 1311-1317), and this method was applied in the arsenic tribromide investigation.

Approximate Structure

Since the least-squares technique applied to electron diffraction is a refinement process (the adjustment if linear only for small ranges of parameter changes), fairly accurate parameters are necessary for the calculation of an initial theoretical intensity curve. This "starting model" is obtained from a representation of the experimental

curve, its Fourier transform, which may be directly analyzed for the magnitudes of the internuclear distances and root-mean-square amplitudes of vibration. This Fourier transform is called a "radial distribution" curve and is calculated from a modified form of the molecular intensity curve, $I'_m(s)$ (37, p. 671-690):

$$I'_m(s) = \sum_{i,j}{}' \frac{M_{ij}}{r_{ij}} e^{-l_{ij}^2 s^2/2} \sin sr_{ij} \qquad (20)$$

$I'_m(s)$ may be obtained for arsenic tribromide from $I_m(s)$ (Equation 19) by multiplying $I_m(s)$ by

$$sZ_{As}Z_{Br}/(Z-f)_{As}(Z-f)_{Br}$$

giving

$$I'_m(s) = 3 \frac{M_{As-Br}}{r_{As-Br}} e^{-l_{As-Br}^2 s^2/2} \sin sr_{As-Br} + 3 \frac{M_{Br\ldots Br}}{r_{Br\ldots Br}} e^{-l_{Br\ldots Br}^2 s^2/2} \sin sr_{Br\ldots Br} \qquad (21)$$

where

$$M_{As-Br} = Z_{As} Z_{Br} \qquad (22)$$

$$M_{Br\ldots Br} = \frac{Z_{As}Z_{Br}(Z-f)_{Br}}{(Z-f)_{As}} \quad . \qquad (23)$$

$M_{Br\ldots Br}$ differs from constancy only as the ratio $\frac{(Z-f)_{Br} Z_{As}}{(Z-f)_{As} Z_{Br}}$ differs from unity. This ratio was calculated and found to be very nearly equal to one over the s ranges used in the analyses. The radial distribution curve may be defined by

TABLE 7. Atom Form Factors for Arsenic and Bromine Tabulated by Hanson (21).

s	f_{As}	f_{Br}	s	f_{As}	f_{Br}
0.00	33.00	35.00	10.00	10.98	12.24
0.25	32.85	34.85	10.25	10.68	11.90
0.50	32.56	34.57	10.50	10.38	11.58
0.75	32.02	34.06	10.75	10.12	11.27
1.00	31.39	33.40	11.00	9.84	10.97
1.25	30.60	32.62	11.25	9.60	10.68
1.50	29.82	31.75	11.50	9.36	10.41
1.75	28.96	30.88	11.75	9.13	10.15
2.00	28.15	29.90	12.00	8.92	9.89
2.25	27.30	29.01	12.25	8.72	9.65
2.50	26.53	28.07	12.50	8.53	9.42
2.75	25.82	27.20	12.75	8.33	9.21
3.00	25.04	26.38	13.00	8.17	9.00
3.25	24.37	25.55	13.25	8.01	8.81
3.50	23.65	24.85	13.50	7.86	8.61
3.75	23.02	24.11	13.75	7.70	8.43
4.00	22.37	23.48	14.00	7.58	8.26
4.25	21.73	22.84	14.25	7.43	8.11
4.50	21.15	22.24	14.50	7.33	7.94
4.75	20.56	21.66	14.75	7.20	7.81
5.00	20.00	21.10	15.00	7.10	7.66
5.25	19.42	20.54	15.25	6.97	7.53
5.50	18.88	20.04	15.50	6.89	7.40
5.75	18.31	19.50	15.75	6.79	7.29
6.00	17.80	19.03	16.00	6.71	7.17
6.25	17.24	18.51	16.25	6.62	7.06
6.50	16.77	18.06	16.50	6.54	6.96
6.75	16.24	17.56	16.75	6.44	6.86
7.00	15.78	17.12	17.00	6.38	6.76
7.25	15.30	16.63	17.25	6.30	6.67
7.50	14.83	16.21	17.50	6.23	6.59
7.75	14.41	15.75	17.75	6.16	6.51
8.00	13.95	15.34	18.00	6.10	6.43
8.25	13.55	14.89	18.25	6.03	6.35
8.50	13.11	14.50	18.50	5.97	6.28
8.75	12.74	14.08	18.75	5.91	6.21
9.00	12.34	13.70	19.00	5.85	6.14
9.25	11.97	13.32	19.25	5.79	6.08
9.50	11.63	12.95	19.50	5.73	6.02
9.75	11.30	12.58	19.75	5.67	6.96

TABLE 7. Continued.

s	f_{As}	f_{Br}	s	f_{As}	f_{Br}
20.00	5.62	5.90	30.00	3.67	4.01
20.25	5.56	5.84	30.25	3.62	3.97
20.50	5.51	5.78	30.50	3.58	3.93
20.75	5.45	5.72	30.75	3.54	3.88
21.00	5.40	5.67	31.00	3.50	3.84
21.25	5.34	5.62	31.25	3.45	3.80
21.50	5.29	5.57	31.50	3.41	3.76
21.75	5.24	5.52	31.75	3.37	3.72
22.00	5.19	5.46	32.00	3.33	3.68
22.25	5.14	5.41	32.25	3.29	3.64
22.50	5.10	5.36	32.50	3.25	3.60
22.75	5.04	5.31	32.75	3.22	3.56
23.00	5.00	5.26	33.00	3.18	3.52
23.25	4.94	5.21	33.25	3.14	3.48
23.50	4.89	5.17	33.50	3.10	3.44
23.75	4.84	5.12	33.75	3.06	3.40
24.00	4.79	5.08	34.00	3.03	3.37
24.25	4.74	5.04	34.25	2.99	3.33
24.50	4.69	4.99	34.50	2.95	3.29
24.75	4.64	4.94	34.75	2.92	3.25
25.00	4.59	4.89	35.00	2.89	3.22
25.25	4.54	4.84	35.25	2.85	3.18
25.50	4.50	4.80	35.50	2.82	3.15
25.75	4.45	4.75	35.75	2.78	3.11
26.00	4.40	4.71	36.00	2.75	3.08
26.25	4.34	4.67	36.25	2.72	3.04
26.50	4.31	4.62	36.50	2.69	3.01
26.75	4.26	4.58	36.75	2.66	2.97
27.00	4.21	4.53	37.00	2.63	2.94
27.25	4.16	4.48	37.25	2.60	2.94
27.50	4.12	4.44	37.50	2.57	2.87
27.75	4.07	4.40	37.75	2.53	2.84
28.00	4.03	4.35	38.00	2.50	2.81
28.25	3.98	4.31	38.25	2.47	2.78
28.50	3.93	4.27	38.50	2.45	2.75
28.75	3.89	4.22	38.75	2.42	2.72
29.00	3.84	4.18	39.00	2.40	2.69
29.25	3.80	4.14	39.25	2.37	2.67
29.50	3.75	4.10	39.50	2.35	2.64
29.75	3.71	4.05	39.75	2.32	2.61

TABLE 8. Atom Form Factors for Arsenic and Bromine Tabulated by Ibers (25. p. 201-227).

s	f_{As}	f_{Br}	s	f_{As}	f_{Br}
.25	32.82	34.93	10.25	11.00	11.86
.50	32.52	34.55	10.50	10.76	11.61
.75	31.93	33.87	10.75	10.55	11.36
1.00	31.19	33.08	11.00	10.33	11.13
1.25	30.37	32.22	11.25	10.12	10.91
1.50	29.48	31.27	11.50	9.91	10.68
1.75	28.52	30.25	11.75	9.73	10.48
2.00	27.48	29.22	12.00	9.53	10.28
2.25	26.50	28.27	12.25	9.34	10.08
2.50	25.58	27.33	12.50	9.16	9.88
2.75	24.73	26.44	12.75	8.98	9.70
3.00	23.96	25.61	13.00	8.82	9.52
3.25	23.21	24.78	13.25	8.66	9.35
3.50	22.50	24.02	13.50	8.50	9.18
3.75	21.81	23.30	13.75	8.35	9.02
4.00	21.12	22.60	14.00	8.20	8.86
4.25	20.48	21.93	14.25	8.06	8.70
4.50	19.84	21.29	14.50	7.93	8.56
4.75	19.23	20.67	14.75	7.79	8.41
5.00	18.67	20.05	15.00	7.65	8.26
5.25	18.17	19.46	15.25	7.52	8.12
5.50	17.67	18.90	15.50	7.40	8.00
5.75	17.20	18.37	15.75	7.28	7.87
6.00	16.75	17.87	16.00	7.16	7.74
6.25	16.30	17.41	16.25	7.05	7.61
6.50	15.84	16.96	16.50	6.92	7.49
6.75	15.41	16.52	16.75	6.82	7.37
7.00	15.00	16.08	17.00	6.71	7.26
7.25	14.61	15.67	17.25	6.61	7.15
7.50	14.23	15.28	17.50	6.51	7.03
7.75	13.88	14.90	17.75	6.40	6.93
8.00	13.53	14.52	18.00	6.31	6.83
8.25	13.21	14.18	18.25	6.21	6.73
8.50	12.88	13.86	18.50	6.11	6.63
8.75	12.58	13.53	18.75	6.01	6.53
9.00	12.30	13.24	19.00	5.92	6.43
9.25	12.02	12.94	19.25	5.86	6.34
9.50	11.75	12.66	19.50	5.77	6.25
9.75	11.48	12.38	19.75	5.71	6.17
10.00	11.23	12.12			

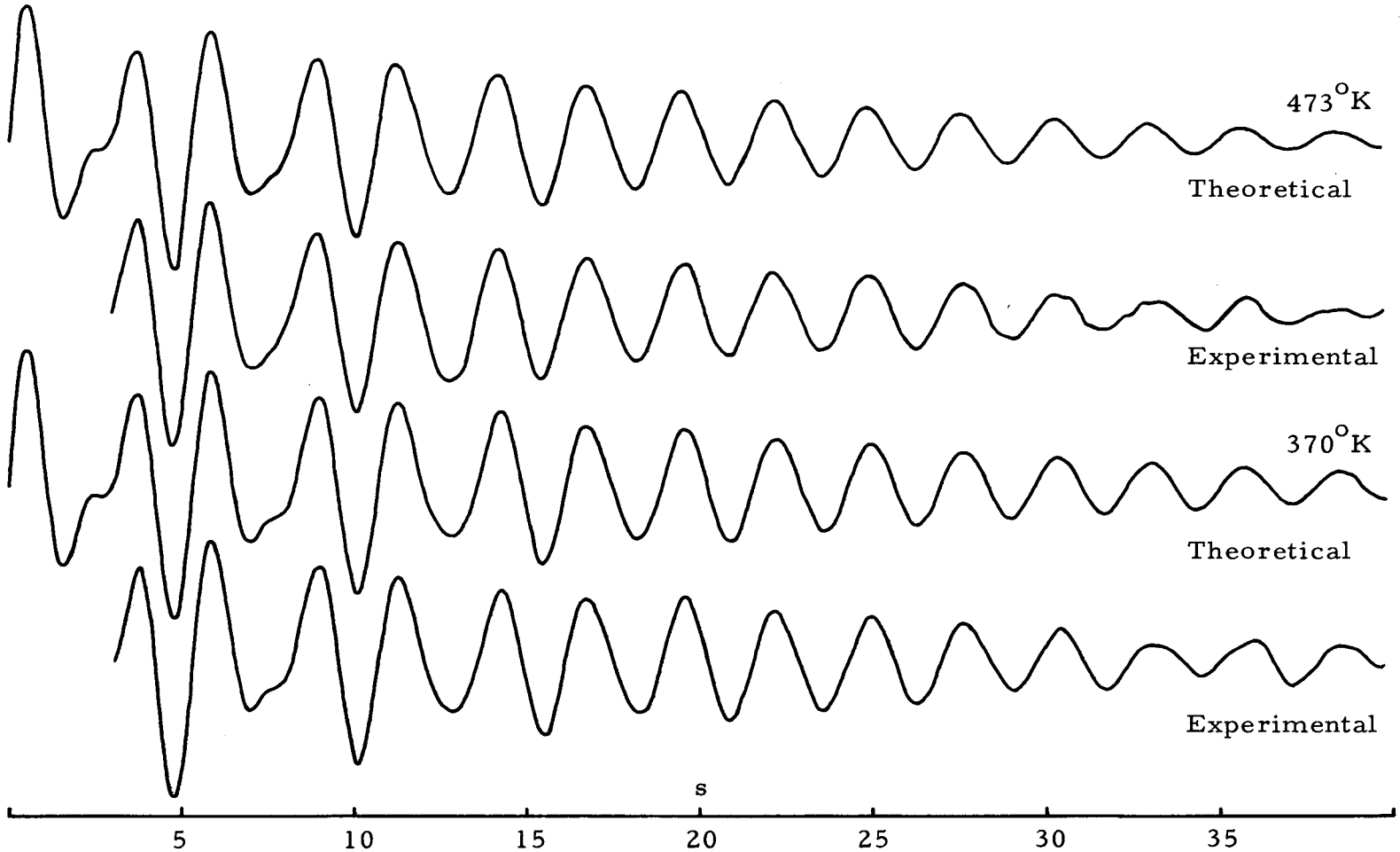

FIGURE 10. Experimental and Theoretical Modified Molecular Intensity Curves, $I'_m(s)$, for Arsenic tribromide.

TABLE 9. Modified Molecular Intensity Curves, $I'_m(s)$, For Arsenic Tribromide.*

	370°K		473°K			370°K		473°K	
s	Exp.	Theo.	Exp.	Theo.	s	Exp.	Theo.	Exp.	Theo.
.00		0.00		0.00	10.00	-55.94	-57.96	-53.64	-52.95
.25		54.00		53.99	10.25	-55.69	-58.20	-51.27	-51.67
.50		79.16		79.06	10.50	-30.50	-32.96	-29.12	-28.93
.75		64.40		64.19	10.75	5.32	4.29	2.17	3.59
1.00		22.12		21.91	11.00	34.73	35.50	26.88	31.05
1.25		-21.56		-21.59	11.25	47.78	48.24	40.58	43.31
1.50		-44.49		-44.31	11.50	41.07	41.09	38.43	38.75
1.75		-41.55		-41.34	11.75	20.64	21.81	21.16	22.83
2.00		-24.43		-24.44	12.00	1.16	0.81	4.06	3.37
2.25		- 9.73		-10.00	12.25	-14.26	-15.10	-13.58	-13.63
2.50		- 5.35		- 5.58	12.50	-24.37	-24.48	-24.06	-25.31
2.75		- 5.76		- 5.50	12.75	-28.44	-28.77	-28.89	-30.72
3.00	-3.67	0.86	1.62	1.71	13.00	-28.18	-28.51	-27.65	-29.08
3.25	14.06	19.99	20.88	20.90	13.25	-22.29	-22.05	-19.24	-19.65
3.50	34.69	43.34	42.09	43.47	13.50	-8.97	-7.70	-4.64	-3.22
3.75	52.74	53.30	55.01	52.15	13.75	10.61	12.73	14.85	16.32
4.00	37.31	36.25	37.27	34.26	14.00	30.88	32.53	30.77	33.25
4.25	-3.65	-5.26	-7.27	-6.82	14.25	40.04	42.52	36.58	37.70
4.50	-51.99	-51.30	-54.90	-51.13	14.50	34.94	36.31	28.76	29.30
4.75	-78.85	-75.92	-76.50	-73.82	14.75	11.57	14.73	6.11	9.51
5.00	-65.53	-63.87	-59.76	-61.03	15.00	-15.57	-13.67	-13.86	-14.04
5.25	-20.66	-20.77	-19.64	-19.08	15.25	-36.04	-36.67	-33.98	-32.01
5.50	31.93	30.19	29.72	29.53	15.50	-43.76	-44.61	-37.44	-37.62
5.75	64.05	62.72	60.40	60.13	15.75	-34.18	-35.04	-26.95	-29.47
6.00	65.18	63.07	59.51	60.41	16.00	-11.00	-13.27	- 8.72	-11.63
6.25	38.78	36.63	33.09	35.76	16.25	13.13	10.99	10.54	8.74
6.50	5.56	1.78	1.48	3.17	16.50	29.11	28.68	23.39	24.53
6.75	-20.17	-23.33	-23.47	-21.03	16.75	34.56	34.94	31.08	31.23
7.00	-29.02	-31.51	-31.29	-30.37	17.00	29.55	29.89	26.96	27.82
7.25	-24.34	-27.78	-30.67	-28.85	17.25	14.73	17.01	15.71	16.30
7.50	-19.19	-21.80	-24.02	-24.14	17.50	-1.69	0.79	-1.75	0.57
7.75	-15.64	-18.50	-19.30	-19.87	17.75	-16.08	-14.67	-16.32	-14.75
8.00	-11.75	-14.67	- 6.67	-13.31	18.00	-26.70	-25.94	-24.00	-25.31
8.25	1.33	-3.46	4.29	0.20	18.25	-30.02	-30.23	-27.56	-28.03
8.50	23.69	17.16	22.80	20.58	18.50	-28.09	-25.78	-21.76	-21.94
8.75	44.62	39.73	39.69	40.03	18.75	-14.74	-12.93	- 9.22	-8.75
9.00	53.11	50.63	46.04	46.84	19.00	8.63	5.05	6.96	7.39
9.25	42.38	39.36	32.67	33.49	19.25	23.60	22.30	20.49	21.10
9.50	8.54	7.20	2.52	3.00	19.50	33.22	32.41	26.89	27.65
9.75	-29.31	-31.72	-31.02	-31.30	19.75	32.54	31.16	28.07	24.75

*These curves are composite curves formed by joining the 19 cm and 48 cm curves.

TABLE 9. Continued.

	370°K		473°K			370°K		473°K	
s	Exp.	Theo.	Exp.	Theo.	s	Exp.	Theo.	Exp.	Theo.
20.00	17.34	18.68	15.00	13.51	30.00	11.01	11.76	7.37	8.90
20.25	-2.41	-0.42	-2.25	-2.01	30.25	16.21	16.70	11.41	11.76
20.50	-21.59	-18.91	-18.23	-16.33	30.50	17.49	16.02	9.69	10.69
20.75	-32.79	-30.07	-22.97	-24.64	30.75	12.39	10.15	8.69	6.21
21.00	-32.14	-30.33	-24.33	-24.42	31.00	2.81	1.18	2.56	-0.06
21.25	-21.18	-20.35	-11.68	-16.23	31.25	-5.65	-7.83	-7.11	-6.02
21.50	-3.45	-4.33	0.00	-3.14	31.50	-14.21	-13.96	-8.07	-9.75
21.75	12.98	12.03	11.87	10.35	31.75	-17.14	-15.34	-9.03	-10.16
22.00	25.84	23.53	21.52	19.91	32.00	-14.36	-11.70	-6.92	-7.26
22.25	27.01	27.08	22.91	22.70	32.25	-6.60	-4.42	-2.01	-2.17
22.50	18.47	22.17	17.01	18.15	32.50	2.07	4.00	-0.78	3.38
22.75	5.88	10.69	9.79	7.98	32.75	6.67	10.82	6.72	7.56
23.00	-7.90	-3.74	-4.93	-4.40	33.00	8.38	13.91	6.12	9.10
23.25	-22.53	-16.76	-16.15	-14.97	33.25	7.58	12.38	6.94	7.62
23.50	-29.38	-24.39	-21.28	-20.40	33.50	8.46	6.90	6.34	3.76
23.75	-26.56	-24.20	-18.90	-19.07	33.75	3.83	-0.61	2.39	-1.12
24.00	-16.26	-16.17	-11.43	-11.58	34.00	-1.28	-7.63	-3.53	-5.38
24.25	-3.41	-2.85	0.00	-0.56	34.25	-7.73	-11.91	-5.68	-7.70
24.50	10.99	11.34	14.17	10.30	34.50	-9.92	-12.17	-9.05	-7.41
24.75	21.79	21.59	19.45	17.43	34.75	-6.50	-8.49	-9.75	-4.75
25.00	24.37	24.43	20.88	18.60	35.00	0.00	-2.21	-3.76	-0.70
25.25	17.87	19.02	17.08	13.66	35.25	3.50	4.54	0.98	3.36
25.50	7.06	7.39	6.62	4.46	35.50	6.16	9.55	6.43	6.12
25.75	-8.17	-6.32	-7.99	-5.83	35.75	9.72	11.27	9.28	6.76
26.00	-20.74	-17.44	-14.75	-13.80	36.00	11.10	9.28	8.16	5.19
26.25	-25.54	-22.38	-20.23	-16.96	36.25	9.82	4.37	1.50	2.04
26.50	-21.73	-19.82	-17.65	-14.49	36.50	0.00	-1.75	-2.52	-1.60
26.75	-13.49	-10.95	-9.57	-7.43	36.75	-6.76	-7.05	-5.24	-4.53
27.00	0.00	1.07	0.00	1.73	37.00	-15.84	-9.85	-5.26	-5.83
27.25	12.91	12.27	9.67	9.93	37.25	-13.19	-9.35	-4.09	-5.19
27.50	19.67	19.12	16.70	14.60	37.50	-9.14	-5.86	-2.57	-2.91
27.75	20.91	19.63	15.41	14.36	37.75	-3.67	-0.62	0.52	0.17
28.00	15.78	13.84	13.68	9.48	38.00	3.69	4.59	0.69	3.02
28.25	3.40	3.80	5.67	1.74	38.25	6.95	8.10	1.56	4.74
28.50	-3.80	-7.17	-7.13	-6.23	38.50	9.78	8.84	1.92	4.83
28.75	-12.61	-15.53	-11.46	-11.84	38.75	6.55	6.69	1.75	3.37
29.00	-17.68	-18.64	-14.41	-13.37	39.00	4.70	2.48	0.35	0.90
29.25	-15.47	-15.61	-14.50	-10.51	39.25	0.00	-2.34	-1.42	-1.70
29.50	-8.17	-7.58	-5.83	-4.38	39.50	-4.74	-6.20	-0.18	-3.61
29.75	0.00	2.69	0.00	2.89	39.75	-3.81	-7.88	1.60	-4.24

$$\frac{P_{(r)}}{r} = \int_0^\infty I'_m(s) \sin(rs)\, ds \tag{24}$$

from which, using $I'_m(s)$ from equation (20)

$$\frac{P_{(r)}}{r} = \sum_{i,j}{}' \frac{Z_i Z_j}{4 r_{ij}} \left(\frac{2\pi}{l_{ij}^2}\right)^{1/2} e^{-(r-r_{ij})/2l_{ij}^2} \tag{25}$$

$\frac{P_{(r)}}{r}$ is thus a curve consisting of a sum of curves, each a Gaussian, whose peak position gives an internuclear distance and whose dispersion is related to the root-mean-square amplitude of vibration l_{ij} (9, p. 256-257). The radial distribution curves for arsenic tribromide were actually calculated by the approximate relation

$$\frac{P_{(n)}}{r} \approxeq \sum_{\substack{s = 0.25, \\ 0.50, \cdots}}^{s = 40.00} I'_m(s)\, e^{-as^2} \sin rs \tag{26}$$

where the term e^{-as^2} was included to provide for better convergence of the series. Intensity values at small s, missing in $I'_m(s)$, were sketched in from a preliminary theoretical curve and improved values consistent with the final results were introduced as the analysis proceeded (26, p. 2239-2245). In principle, a radial distribution curve should have no negative values, or at most only small negative values. Such negative values do in fact appear in electron diffraction work and are generally ascribable to errors in placement of the

experimental background used to derive $I'_m(s)$. Corrections to this experimental background are obtained from the indications of the radial distribution curve, and upon incorporation lead to an "improved" $I_m(s)$, and in turn to an improved radial distribution curve. This procedure was necessary in the arsenic tribromide analysis, and was applied to data from both camera distances at each temperature (6, p. 813-821).

Figure 11 shows the final radial distribution curves for arsenic tribromide. Each curve is the result of a calculation in which data from both the 19 cm and 48 cm camera distance experiments were combined to form a composite intensity curve.[1] Values of the internuclear distances and mean amplitudes of vibration from the radial distribution curves are shown in Table 12.

Refinement of Structure

The least-squares procedure mentioned at the beginning of this section was applied to refinement of the structure using starting models having parameter values near to those of Table 12. A large number of refinements were carried out, differing in such things as

[1]The composite curves were formed by a simple averaging of data in the region of overlap. Since the data from the two camera distances were on arbitrary scales, an amplitude scale adjustment had to be applied to data from one of them. This was done by use of a scale factor evaluated either by least-squares or by a simple averaging of selected data in the region of overlap.

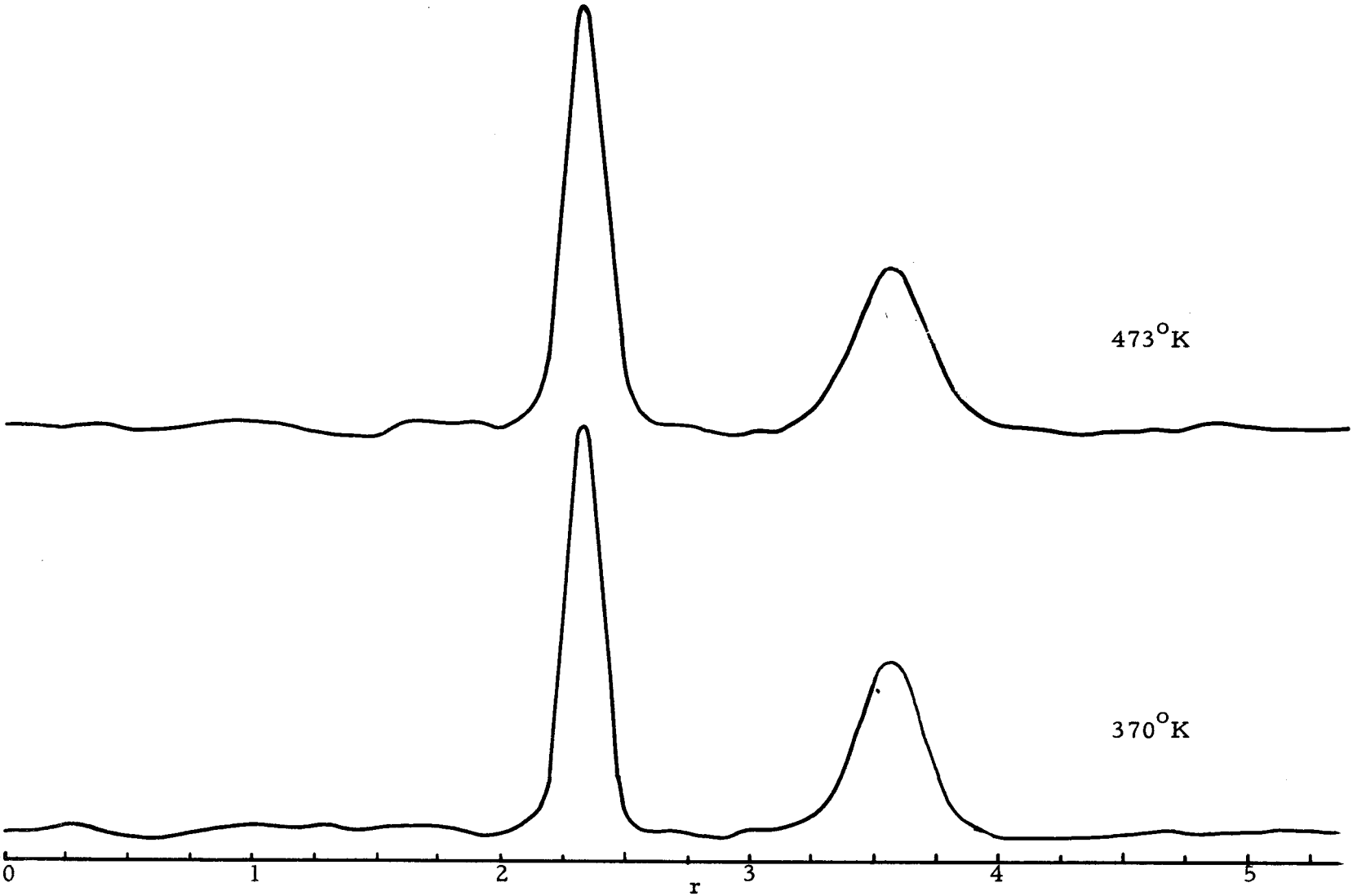

FIGURE 11. Radial Distribution Curves for Arsenic Tribromide (in Angstroms).

TABLE 10. Radial Distribution Curves for Arsenic Tribromide.

r	370°K	473°K	r	370°K	473°K	r	370°K	473°K
0.05	-1.3	0.1	2.05	5.6	4.3	4.05	-4.0	1.4
0.10	2.3	-0.6	2.10	11.1	12.3	4.10	-5.6	1.4
0.15	9.1	-2.3	2.45	19.2	27.0	4.15	-6.1	0.6
0.20	13.4	-3.7	2.20	79.3	93.6	4.20	-6.1	-1.2
0.25	10.6	-2.5	2.25	229.2	236.7	4.25	-5.8	-2.8
0.30	3.5	0.9	2.30	384.1	378.7	4.30	-4.8	-4.8
0.35	-3.0	3.0	2.35	397.7	397.8	4.35	-3.5	-6.1
0.40	-5.8	1.5	2.40	260.0	280.0	4.40	-3.8	-4.6
0.45	-7.8	-1.5	2.45	103.9	133.1	4.45	-3.8	-1.9
0.50	-11.9	-3.0	2.50	22.0	46.0	4.50	-1.7	-0.8
0.55	-16.4	-2.4	2.55	-0.8	15.2	4.55	-0.3	-1.4
0.60	-17.7	-0.6	2.60	-2.8	5.6	4.60	-0.0	-3.1
0.65	-13.4	0.5	2.65	-0.5	2.8	4.65	1.0	-4.6
0.70	-6.0	0.0	2.70	-2.8	1.5	4.70	2.3	-3.2
0.75	-0.7	-0.1	2.75	-7.1	-1.4	4.75	0.8	0.5
0.80	0.5	1.4	2.80	-6.1	-2.8	4.80	0.3	2.8
0.85	1.3	3.2	2.85	-3.5	-3.4	4.85	2.0	3.4
0.90	4.5	4.3	2.90	-2.3	-6.5	4.90	4.0	3.9
0.95	7.1	4.9	2.95	1.5	-8.0	4.95	3.3	3.7
1.00	5.3	4.4	3.00	2.8	-5.4	5.00	3.5	2.4
1.05	3.0	2.3	3.05	1.0	-4.1	5.05	4.5	1.4
1.10	4.0	0.2	3.10	2.0	-3.8	5.10	2.5	1.1
1.15	4.5	-1.4	3.15	6.8	1.8	5.15	0.5	0.8
1.20	2.3	-2.9	3.20	10.1	11.2	5.20	1.8	0.3
1.25	3.3	-3.7	3.25	14.2	20.3	5.25	3.8	0.0
1.30	6.5	-4.5	3.30	27.3	33.7	5.30	3.3	0.0
1.35	4.5	-6.0	3.35	46.7	55.7	5.35	1.8	0.5
1.40	-0.3	-6.7	3.40	76.1	82.5	5.40	1.3	1.0
1.45	-0.3	-6.0	3.45	115.5	110.7	5.45	0.8	1.4
1.50	2.0	-3.2	3.50	152.9	137.5	5.50	0.5	2.4
1.55	2.8	2.8	3.55	170.4	153.8	5.55	-1.3	3.1
1.60	4.8	8.4	3.60	161.0	150.0	5.60	-1.5	2.3
1.65	6.6	7.9	3.65	131.4	128.1	5.65	-2.0	1.1
1.70	3.3	3.1	3.70	93.2	97.8	5.70	-2.3	0.1
1.75	0.0	1.2	3.75	56.9	67.5	5.75	-2.0	-1.3
1.80	0.5	2.0	3.80	28.8	42.2	5.80	-1.8	-3.0
1.85	-1.0	0.9	3.85	11.9	25.1	5.85	-2.3	-3.9
1.90	-5.3	-2.4	3.90	4.0	15.6	5.90	-2.3	-4.0
1.95	-6.1	-5.6	3.95	1.3	9.2	5.95	-1.0	3.0
2.00	-2.0	-4.0	4.00	-1.3	3.9	6.00	0.3	-2.1

(1) the type of intensity curve used [$I'_m(s)$ or $I_m(s)$], (2) the tabulated values of the atom form factor, f_i, (which appear in the calculation either explicitly [$I_m(s)$] or, having been divided out implicitly [$I'_m(s)$], and which depend on the atomic potential assumed in their derivation), (3) the blackness correction used in data reduction, (4) the s range of the intensity curves (that is, long or short camera distance data), and (5) the amplitude scale adjustment of 48 cm and 19 cm intensity data to give the composite curve. The results of these refinements are summarized in Table 11.

Evaluation of Errors

The errors derived solely from the results of the least-squares analyses do not reflect the effect of any systematic errors such as might occur in measurements of the electron wave length, the camera distances, or the trace-plate ratio of position coordinate; of errors in the blackness correction, the sector correction, amplitude scale adjustments, or in the atom form factors. Further, as Morino has recently pointed out[1], the experimental intensity curves are not measured quantities but composites of data, a fact which introduces still another kind of error which will be designated as σ_p. Plausible estimates of these errors may be made as follows:

---

[1]Morino, Yonezo. Private communication. Tokyo, Japan. University of Tokyo, 1964.

1. Electron wave lengths, camera distance and position coordinate: Errors in these quantities affect largely the size of the molecule and are of no consequence in the determination of the vibrational amplitudes. An examination of the variation of wave length over a period of several months, and of the camera distance measuring procedure suggest these errors to be about 0.0005 r_{ij} (22, p. 593); in comparison, the error in the position coordinate is negligible.

2. Blackness correction, sector correction, scale adjustment, and atom form factors: Errors in these quantities affect largely the amplitudes of vibration. They may be estimated by comparing the differences in mean amplitude values gotten from the analysis of curves in which these quantities have been combined in as many different ways as possible. The mean amplitude values to be considered are thus just those to be found in Table 12. For example, at the low temperature, the l_{As-Br} values from column HGF (I'_m) and HO (I'_m) average to 0.04903 Å, leading to a standard error due to the blackness correction. $\sigma_B(As-Br) = 0.0012$ Å; for $l_{Br...Br}$ the corresponding calculation gives $\sigma_B(Br...Br) = 0.0013$ Å. These values and those obtained by a similar procedure for the atom form factors, amplitude scale adjustments, and type of intensity curve (the sector correction error is a completely unknown quantity) are given in Table 15.

TABLE 11. Results of Least-Squares Refinements (In Å).

	370° K							
	HGF				HO			
	48 cm	19 cm	$I_m'(s)$	$I_m(s)$	48 cm	19 cm	I'_m	$I'^{(a)}_m$
r_{As-Br}	2.327_0	2.329_0	2.328_0	2.329_0	2.326_5	2.329_5	2.328_0	2.328_0
$r_{Br...Br}$	3.555_0	3.571_0	3.559_5	3.561_0	3.556_5	3.572_5	3.565_5	3.558_5
l_{As-Br}	0.048_7	0.047_3	0.048_2	0.047_9	0.054_0	0.049_5	0.050_7	0.049_9
$l_{Br...Br}$	0.117_1	0.107_2	0.114_0	0.113_2	0.117_7	0.107_2	0.113_9	0.112_2

	370°K						473°K			
	IGF			IO			HGF			
	48 cm	19 cm	I'_m	48 cm	19 cm	$I'_m(a)$	48 cm	19 cm	$I'^{(a)}_m$	$I^{(a)}_m$
r_{As-Br}	2.328_0	2.329_5	2.328_5	2.327_5	2.329_5	2.328_5	2.330_0	2.331_5	2.331_0	2.331_5
$r_{Br...Br}$	3.555_5	3.570_5	3.561_5	3.555_5	3.570_0	3.567_5	3.563_5	3.558_5	3.563_0	3.562_5
l_{As-Br}	0.027_8	0.047_4	0.045_1	0.035_3	0.050_0	0.046_3	0.057_2	0.049_1	0.055_8	0.055_5
$l_{Br...Br}$	0.107_2	0.106_5	0.108_7	0.107_3	0.106_9	0.113_4	0.136_2	0.127_5	0.136_7	0.135_3

HGF. Results obtained by applying Hanson's factors, gold foil blackness correction
HO. Results obtained by applying Hanson's factors, Oslo blackness correction
IGF. Results obtained by applying Iber's factors, gold foil blackness correction
IO. Results obtained by applying Iber's factors, Oslo blackness correction
(a). Composite curve formed by simple averaging of selected peaks for scale constant

TABLE 12. Distances and RMS Amplitudes from Radial Distribution Curves Assuming Gaussian Peak Shapes (in Å).

	r_{As-Br}	$r_{Br...Br}$	l_{As-Br}	$l_{Br...Br}$
370°K	2.33_0	3.56_0	0.049_0	0.117_0
473°K	2.33_0	3.57_0	0.057_5	0.132_0

TABLE 13. Final Results of Structure Analyses (in Å).

	r_{As-Br}	$r_{Br...Br}$	l_{As-Br}	$l_{Br...Br}$	∠ Br-As-Br
370°K	$2.329 \pm .002$	$3.561 \pm .005$	$.047_9 \pm .004_5$	$.113_2 \pm .005_3$	$99.6_6 \pm .2_6$
473°K	$2.332 \pm .002$	$3.563 \pm .005$	$.055_5 \pm .004_5$	$.135_3 \pm .005_3$	$99.7_2 \pm .2_9$

TABLE 14. Effect of Temperature on the Root-Mean-Square Amplitudes of Vibration of Arsenic Tribromide.

	Calc.	$l_{As-Br}^{(obs)}$	$l_{Br...Br}^{(obs)}$
l_{ij} (473)/l_{ij} (370)	1.13	1.15	1.19

3. Composite data: Errors from this source were not estimated from the arsenic tribromide data themselves. Although it would have been possible to do so, the procedure is long, requiring analyses of each plate similar to that described above for the composite data from all plates. It was decided, therefore, to use results obtained earlier by Mr. Jerome S. Blank[1] in this laboratory for the molecule nitrogen dioxide. The data for this molecule and for arsenic tribromide are comparable in extent, and other factors which could conceivably affect the error seem also to be comparable. The σ_p values obtained by Mr. Blank based on 19 cm data are respectively 0.009 Å, 0.0030 Å, 0.0014 Å, and 0.0009 Å for r_{N-O}, $r_{O...O}$, l_{N-O} and $l_{O...O}$. These were adapted as the σ_p values for r_{As-Br}, $r_{Br...Br}$, l_{As-Br} and $l_{Br...Br}$, respectively.

The estimates of overall standard errors associated with each parameter are given in Table 13. These were obtained as follows. For each distance at each temperature the estimated standard error $\sigma_\lambda (r_{ij}) = .0005\ r_{ij}$ arising from the measured uncertainties in the electron wave length, camera distance and position coordinate, and the σ_p values listed above were combined with the standard error

---

[1]Blank, Jerome S. Unpublished research on molecular structure of nitrogen dioxide. Corvallis, Oregon. Oregon State University, Department of Chemistry, 1964.

TABLE 15. Results of Error Analyses (in Å).

	l_{As-Br}	$l_{Br...Br}$	r_{As-Br}	$r_{Br...Br}$
A	$0.049_0 \pm .001_2$	$0.113_0 \pm .001_3$		
B	$0.047_5 \pm .003_8$	$0.112_5 \pm .003_8$		
C	$0.050_5 \pm .006_0$	$0.113_0 \pm .001_3$		
D	$0.048_0 \pm .002_0$	$0.113_5 \pm .000_6$		
E	$0.047_9 \pm .001_1$	$0.113_2 \pm .002_9$	$2.329 \pm .000_8$	$3.561 \pm .003_5$
F	$0.055_5 \pm .001_0$	$1.135_0 \pm .003_1$	$2.332 \pm .000_8$	$3.563 \pm .003_8$
G			$2.329 \pm .001_2$	$3.56_0 \pm .001_8$
H			$2.331 \pm .001_2$	$3.562_5 \pm .001_8$

A: Effect of blackness correction (gold foil or Oslo)
B: Effect of atom form factors (Iber's or Hanson's)
C: Effect of amplitude scale adjustment procedure
D: Effect of type of intensity curve ($I'_m(s)$ or $I_m(s)$)
E: Least-squares values at 370°K
F: Least-squares values at 473°K
G: Effect due to errors in wave length, camera distance, 370°K
H: Effect due to errors in wave length, camera distance, 473°K

$\sigma_{ls}(r_{ij})$ gotten from the least-squares refinements, according to the relation

$$\sigma_T(r_{ij}) = (\sigma^2_\lambda(r_{ij}) + 2\,\sigma^2_{ls}(r_{ij}) + \sigma^2_p(r_{ij}))^{1/2} \quad . \tag{27}$$

The $\sigma_{ls}(r_{ij})$ values are the square roots of the diagonal elements of the error matrices (Tables 16a and 16b) described below; the factor of two was included as a rough estimate of the effect of correlation among the observed data (23, p. 597). In a similar manner an overall standard error for each vibrational amplitude was determined from

$$\sigma_T(l_{ij}) = (\sigma^2_{exp}(l_{ij}) + 2\,\sigma^2_{ls}(l_{ij}) + \sigma^2_p(l_{ij}))^{1/2} \tag{28}$$

where $\sigma^2_{exp}(l_{ij})$ is

$$\sigma^2_{exp}(l_{ij}) = \sigma^2_B(l_{ij}) + \sigma^2_F(l_{ij}) + \sigma^2_s(l_{ij}) + \sigma^2_I(l_{ij}) \quad .$$

$\sigma_B(l_{ij})$, $\sigma_F(l_{ij})$, $\sigma_s(l_{ij})$, $\sigma_I(l_{ij})$ are the standard errors gotten from the uncertainties in the blackness correction, atom form factors, amplitude scale adjustments, and type of molecular intensity curves, respectively, by the procedures outlined above and listed in Table 15.

Final Results

The final values of the structural parameters with estimated standard errors are given in Table 13. The parameter values themselves are those of $I_m(s)$ from Table 11, a choice which is to some extent arbitrary. This choice was made for the following reasons. First, the atom form factors used in the calculation of these values

led to more consistent results for the 48 cm, 19 cm, and the composite curves (compare, for example, l_{As-Br} from columns HGF and IGF). Second, the blackness correction derived from the gold foil experiments presumably reflects the effect of photographic procedures employed at about the time that the arsenic tribromide pictures were made; the "Oslo blackness correction", being a composite of results attained over many years is less desirable. On the other hand, it must be admitted that the gold foil experiments are less directly comparable with gas diffraction experiments--it might be, for example, that the response of the photographic plates for equal exposure (exposure equals intensity times time) is different for different exposure time. At any rate, the results using the gold foil blackness correction appear to be more consistent than those obtained using the Oslo correction (compare l_{As-Br} from columns HGF and HO). Third, the least-squares criterion for establishing the scale of the two components of the composite curve would appear to be more reasonable that the simple average criterion.

The standard errors listed in Table 13 have been discussed in the preceding section, except for that associated with the bond angle. Since this parameter is not a function of the molecular size, it will be unaffected by errors in factors of the first type mentioned above. Nor will it be affected by error in factors of the second type, which are related largely to the amplitudes of vibration. There

remains only the error from the composite data factor. The σ_p (angle) value for this error source is found to be .21 degrees, which gives, after combination with σ_{ls}, the tabulated values of .26 degrees and .29 degrees for the high and low temperatures, respectively.

The error matrices (Tables 16a and 16b) are those derived from the least-squares refinements leading to the results reported in Table 13. The matrices listed, $\mathbb{M}$, are related to those actually gotten from the least-squares refinements, $s^2\mathbb{B}^{-1}$, by the well-known equation

$$\mathbb{M} = s^2\, \mathbb{C}\, \mathbb{B}^{-1}\, \mathbb{C}^{-1}$$

where $\mathbb{C}$ is a transformation matrix connecting the parameters of interest ($r_{As\text{-}Br}$, $r_{Br\ldots Br}$, $l_{As\text{-}Br}$, $l_{Br\ldots Br}$, $\angle$Br-As-Br) to those actually adjusted ($r_{As\text{-}Br}$, $r_{Br\ldots Br}$, $l_{As\text{-}Br}$, $l_{Br\ldots Br}$). The matrices have diagonal elements σ_i^2 and off-diagonal elements $\rho_{ij}\,\sigma_i\,\sigma_j$ where the σ's are standard errors and ρ_{ij} is the correlation coefficient for the errors σ_i and σ_j. The column headings correspond to structural parameters; K is an amplitude scale factor parameter necessary for the least-squares procedure, but of no structural interest.

TABLE 16 a. Error Matrix ($x10^6$) 370°K.

$K^{(a)}$	r_{As-Br} (b)	$r_{Br...Br}$	l_{As-Br}	$l_{Br...Br}$	Br + As-Br (c)
965.6102	.3699	.3319	.1556	.2276	-8.9059
	.3091	-.0040	-.0003	.0101	-18.1711
		6.1122	.0044	-.1151	233.3630
			.5643	.3676	.1862
				4.3322	-4.9797
					173.8244

(a) Dimensionless
(b) Distances and Amplitudes quantities in Angstrom^2
(c) Angle quantities in degrees^2

TABLE 16b. Error Matrix ($x10^6$) 473°K.

$K^{(a)}$	r_{As-Br} (b)	$r_{Br...Br}$	l_{As-Br}	$l_{Br...Br}$	Br - As - Br (c)
.0905	.0037	.0022	.1437	.2230	-.1352
	.2896	-.0066	-.0002	.0106	-17.1316
		7.5985	.0026	-.1611	290.2010
			.4933	.3527	.1094
				4.8974	-6.7603
					210.6010

(a) Dimensionless
(b) Distances and Amplitudes quantities in Angstrom^2
(c) Angle quantities in degrees^2

EFFECT OF TEMPERATURE

The proportionality given in the introduction between the mean-square amplitudes of vibration and the temperature (Equation 8) provides a means of estimating the effect of temperature on the amplitudes through the relation

$$\frac{l_{ij}\ (473^\circ\ K)}{l_{ij}\ (370^\circ\ K)} = \sqrt{\frac{473^\circ\ K}{370^\circ\ K}}$$

The expected and the observed ratios of the root-mean-square amplitudes at temperatures of 370° K and 473° K are given in Table 14. The standard errors associated with the measurement of root-mean-square amplitudes vary from 3.9 to 9.4 percent; consideration of the effect of these errors on the values of the tabulated ratios shows that the differences between the observed and calculated ratios corresponds to an amplitude error of about one standard deviation for $l_{Br\ldots Br}$ and about three-tenths of a standard deviation for $l_{As\text{-}Br}$.

The temperature effect may be seen most easily in comparisons of the radial distribution curves (Figure 11): the peaks in the 473° K curve are clearly broader than those in the 370° K curve reflecting the increase population of the higher-lying vibrational states. The effect is also visible, but less obvious to the inexperienced eye, in the experimental intensity curves (Figure 10). The high frequency component (due to $r_{Br\ldots Br}$) is seen to be less prominent

in the 473° curve than in the 370° curve: the weaker shoulder in the minimum at s = 7 and the broader character of the minimum at s = 13 are notable.

DETERMINATION OF VIBRATIONAL POTENTIAL FUNCTION

Summary of Theory

The most general quadratic vibrational potential function for a molecule may be written

$$2V = \sum_{k,l} f_{k,l} R_k R_l \tag{29}$$

where the f's are the potential constants and the R's are some set of internal coordinates. The kinetic energy and the potential energy above may be conveniently written in matrix form as

$$2V = \mathbb{R}' \mathbf{F}_r \mathbb{R} \tag{30}$$

$$2T = \dot{\mathbf{X}}' \mathbb{M} \dot{\mathbf{X}} \tag{31}$$

where $\mathbb{R}$ is a column matrix of the distance changes, $\dot{\mathbf{X}}$ is the time derivative of the matrix of cartesian coordinates, and $\mathbb{M}$ is a diagonal matrix of the atomic masses; primed symbols denote transposed matrices. It is convenient to introduce the normal coordinate $\mathbb{Q}$ and the symmetry coordinates $\$$ defined by the equations

$$\mathbb{R} = \mathbb{V} \$ \tag{32}$$

$$\$ = \mathbb{L} \mathbb{Q} \tag{33}$$

from which

$$\mathbb{R} = \mathbb{V} \mathbb{L} \mathbb{Q} \quad . \tag{34}$$

The mean square amplitude matrix $\mathbf{\Sigma}_r$ (equation 2) becomes

$$\mathbf{\Sigma}_r = \mathbf{V}\ \mathbf{L}\ \mathbf{\Delta}\ \mathbf{L}'\ \mathbf{V}' \tag{35}$$

$$= \mathbf{U}\ \mathbf{\Delta}\ \mathbf{U}' \tag{2}$$

where $\mathbf{\Delta} = \mathbf{Q}\ \mathbf{Q}'$ is given by equation (3) and $\mathbf{U}$ by

$$\mathbf{U} = \mathbf{V}\ \mathbf{L} \quad . \tag{36}$$

One may relate cartesian and symmetry coordinates by

$$\mathbf{X} = \mathbf{A}\ \mathbf{R} \tag{37}$$

from which equation (31) becomes

$$2T = \dot{\mathbf{R}}'\ \mathbf{A}'\ \mathbf{M}\ \mathbf{A}\ \dot{\mathbf{R}} \tag{38}$$

$$= \dot{\mathbf{R}}'\ \mathbf{G}_r^{-1}\ \dot{\mathbf{R}} \tag{39}$$

and by using equation (34)

$$2T = \dot{\mathbf{Q}}'\ \mathbf{L}'\ \mathbf{V}'\ \mathbf{G}_r^{-1}\mathbf{V}\ \mathbf{L}\ \dot{\mathbf{Q}} \tag{40}$$

$$= \dot{\mathbf{Q}}'\ \mathbf{L}'\ \mathbf{G}_s^{-1}\ \mathbf{L}\ \dot{\mathbf{Q}} \tag{41}$$

$$= \dot{\mathbf{Q}}'\mathbf{E}\ \dot{\mathbf{Q}} \tag{42}$$

where $\mathbf{E}$ is the identity matrix. Further, one obtains from equations (30), (32), and (33)

$$2V = \mathbf{S}'\ \mathbf{V}'\ \mathbf{F}_r\ \mathbf{V}\ \mathbf{S} \tag{43}$$

$$= \mathbf{S}'\ \mathbf{F}_s\ \mathbf{S} \tag{44}$$

$$= \mathbf{Q}'\ \mathbf{L}'\ \mathbf{F}_s\ \mathbf{L}\ \mathbf{Q} \tag{45}$$

$$= \mathbf{Q}'\ \mathbf{\Lambda}\ \mathbf{Q} \tag{46}$$

The vibrational problem may be solved by combining, for example, equation (41) and (45) as follows. From

$$\mathbf{L}'\ \mathbf{G}_s^{-1}\ \mathbf{L} = \mathbf{E} \tag{47}$$

one obtains

$$\mathbb{L}^{-1}\ \mathbb{G}_s\ \mathbb{L}'^{-1} = \mathbb{E} \tag{48}$$

Since

$$\mathbb{L}'\ \mathbb{F}_s\ \mathbb{L} = \Lambda \tag{49}$$

one has

$$\mathbb{L}^{-1}\ \mathbb{G}_s\ \mathbb{L}'^{-1}\ \mathbb{L}'\ \mathbb{F}_s\ \mathbb{L} = \mathbb{E}\,\Lambda$$

$$\mathbb{L}^{-1}\ \mathbb{G}_s\ \mathbb{F}_s\ \mathbb{L} = \Lambda$$

$$\mathbb{G}_s\ \mathbb{F}_s\ \mathbb{L} = \mathbb{L}\,\Lambda \tag{50}$$

This may be written

$$(\mathbb{G}_s\ \mathbb{F}_s - \lambda_i\ \mathbb{E})\ \mathbb{l}_i = 0 \tag{51}$$

where the $\mathbb{l}_i$'s are the eigenvectors of the $\mathbb{G}\ \mathbb{F}$ matrix and λ_i's ($=4\pi^2 \nu_i^2$) are the eigenvalues. The elements of the $\mathbb{L}$ matrix may be obtained from equation (51), together with the normalization condition $\mathbb{G}_s = \mathbb{L}\ \mathbb{L}'$.

Application to Arsenic Tribromide

The arsenic tribromide molecule has point group symmetry C_{3v} (Figure 12). The general quadratic vibrational potential function (equation 29) thus becomes

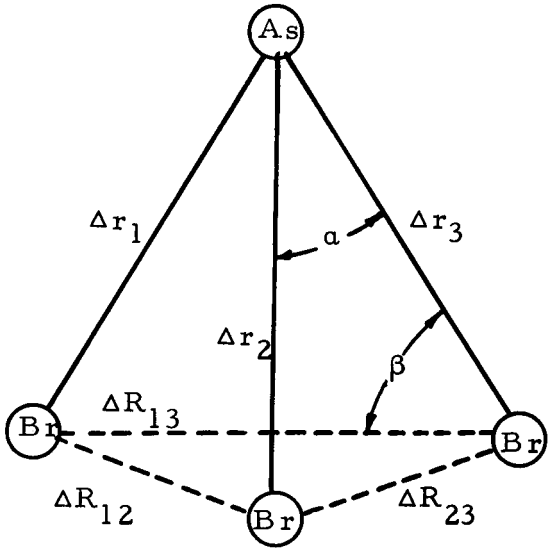

FIGURE 12. Molecular Model of Arsenic Tribromide with Labeling of Internal Coordinates.

$$2V = f_r[(\Delta r_1)^2 + (\Delta r_2)^2 + (\Delta r_3)^2] + f_R[(\Delta R_{12})^2 + (\Delta R_{23})^2 + (\Delta R_{13})^2]$$
$$+ 2 f_{rr}[(\Delta r_1)(\Delta r_2) + (\Delta r_1)(\Delta r_3) + (\Delta r_2)(\Delta r_3)]$$
$$+ 2f_{RR}[(\Delta R_{12})(\Delta R_{23}) + (\Delta R_{12})(\Delta R_{13}) + (\Delta R_{23})(\Delta R_{13})]$$
$$2f_{rR}[(\Delta r_1)(\Delta R_{12}) + (\Delta r_1)(\Delta R_{13}) + (\Delta r_2)(\Delta R_{12})]$$
$$+ (\Delta r_2)(\Delta R_{23}) + (\Delta r_3)(\Delta R_{13}) + (\Delta r_3)(\Delta R_{23})]$$
$$+ 2f_{rR'}[(\Delta r_1)(\Delta R_{23}) + (\Delta r_2)(\Delta R_{13}) + (\Delta r_3)(\Delta R_{12})] \quad . \qquad (52)$$

A convenient set of symmetry coordinates is

$$S_1 = 3^{-1/2}(\Delta r_1 + \Delta r_2 + \Delta r_3)$$
$$S_2 = 3^{-1/2}(\Delta R_{13} + \Delta R_{12} + \Delta R_{23})$$
$$S_3 = 2^{-1/2}(\Delta r_1 - \Delta r_2)$$
$$S_4 = 2^{-1/2}(\Delta R_{31} - \Delta R_{23})$$
$$S_5 = 6^{-1/2}(\Delta r_1 + \Delta r_2 - 2\Delta r_3)$$
$$S_6 = 6^{-1/2}(\Delta R_{12} + \Delta R_{23} - 2\Delta R_{13}) \quad . \qquad (53)$$

The elements of the $\mathbb{V}$ matrix may be written down by inspection, and lead immediately to the elements F_{ij} of the symmetrized $\mathbb{F}$ matrix (equations 43 and 44) and to the elements G_{ij} of the symmetrized $\mathbb{G}$ matrix (equations 39 and 40). These elements are

$$F_{11} = f_r + 2f_{rr}; \quad G_{11} = G_r + 2G_{rr} = \mu_{As} + \mu_{Br} + 2\mu_{As} \cos \alpha$$

$$F_{12} = 2f_{rR} + f_{rR'}; \quad G_{12} = 2G_r + G_{rR'} = 2\mu_{As} \cos \beta$$

$$F_{22} = f_R + 2f_{RR}; \quad G_{22} = G_R + 2G_{RR} = 3\mu_{Br}$$

$$F_{33} = f_r - f_{rr}; \quad G_{33} = G_r = G_{rr} = \mu_{As} + \mu_{Br} = \mu_{As} \cos \alpha$$

$$F_{34} = f_{rR} - f_{rR'}; \quad G_{34} = G_{rR} - G_{rR'} = \mu_{Br} \cos \beta$$

$$F_{44} = f_r - f_{RR}; \quad G_{44} = G_R - G_{RR} = 3/2\ \mu_{Br} \tag{54}$$

where $G_r = \mu_{As} + \mu_{Br}$, $G_{rr} = \mu_{As} \cos \alpha$, $G_{rR} = \mu_{Br} \cos \beta$, $G_{rR'} = 0$ $G_R = 2\mu_{Br}$, and $G_{RR} = 1/2\ \mu_{Br}$; μ_{As} and μ_{Br} are the reciprocal masses of arsenic and bromine. These quantities may be substituted into equation (35) to give

$$l^2_{As\text{-}Br} = \frac{1}{3}(\Delta_1 L^2_{11} + \Delta_2 L^2_{12}) + \frac{2}{3}(\Delta_3 L^2_{33} + \Delta_4 L^2_{34}) \tag{55}$$

$$l^2_{Br \ldots Br} = \frac{1}{3}(\Delta_1 L^2_{21} + \Delta_2 L^2_{22}) + \frac{2}{3}(\Delta_3 L^2_{43} + \Delta_4 L^2_{44}) \tag{56}$$

The secular equation

$$| \mathbb{G}_s \mathbb{F}_s - \lambda_i \mathbb{E} | = 0 \tag{57}$$

together with the normalization condition $\mathbb{L}\ \mathbb{L}' = \mathbb{G}$ lead to the following expressions for the squares of the $\mathbb{L}$ matrix elements.

$$L^2_{11} = \frac{G_{11}\lambda_2^{-1} - F_{11}^{-1}}{\lambda_2^{-1} - \lambda_1^{-1}} \qquad L^2_{33} = \frac{G_{33}\lambda_4^{-1} - F_{33}^{-1}}{\lambda_4^{-1} - \lambda_3^{-1}}$$

$$L^2_{12} = \frac{G_{11}\lambda_1^{-1} + F_{11}^{-1}}{\lambda_2^{-1} - \lambda_1^{-1}} \qquad L^2_{34} = \frac{-G_{33}\lambda_3^{-1} + F_{33}^{-1}}{\lambda_4^{-1} - \lambda_3^{-1}}$$

$$L^2_{21} = \frac{G_{22}\lambda_2^{-1} - F_{22}^{-1}}{\lambda_2^{-1} - \lambda_1^{-1}} \qquad L^2_{43} = \frac{G_{44}\lambda_4^{-1} - F_{44}^{-1}}{\lambda_4^{-1} - \lambda_3^{-1}}$$

$$L^2_{22} = \frac{G_{22}\lambda_1 + F_{22}^{-1}}{\lambda_2^{-1} - \lambda_1^{-1}} \qquad L^2_{44} = \frac{-G_{44}\lambda_3^{-1} + F_{44}^{-1}}{\lambda_4^{-1} - \lambda_3^{-1}} \tag{58}$$

These may be substituted into equation (55) and (56), which together with the four equations resulting from solution of the secular equation serve to relate the experimentally observed mean amplitudes and frequencies to the desired potential constants:

$$l^2_{As\text{-}Br} = \frac{1}{3}(bF_{22} + 2b'F_{44}) + \frac{1}{3}(aG_{11} + 2a'G_{33}) \tag{59}$$

$$l^2_{Br\ldots Br} = \frac{1}{3}(bF_{11} + 2b'F_{33}) + \frac{1}{3}(aG_{22} + 2a'G_{44}) \tag{60}$$

$$\lambda_1 + \lambda_2 = G_{11}F_{11} + 2G_{12}F_{12} + G_{22}F_{22} \tag{61}$$

$$\lambda_1\lambda_2 = (G_{11}G_{22} - G_{12}^2)(F_{11}F_{22} - F_{12}^2) \tag{62}$$

$$\lambda_3 + \lambda_4 = G_{33}F_{33} + 2G_{34}F_{34} + G_{44}F_{44} \tag{63}$$

$$\lambda_3\lambda_4 = (G_{33}G_{44} - G_{34}^2)(F_{33}F_{44} - F_{34}^2) \tag{64}$$

where

$$a = (\Delta_1\lambda_1 - \Delta_2\lambda_2)/(\lambda_1 - \lambda_2)$$

$$a' = (\Delta_3\lambda_3 - \Delta_4\lambda_4)/(\lambda_3 - \lambda_4)$$

$$b = (\Delta_2 - \Delta_1)(G_{11}G_{22} - G_{12}^2)/(\lambda_1 - \lambda_2)$$

$$b' = (\Delta_4 - \Delta_3)(G_{33}G_{44} - G_{34}^2)/(\lambda_3 - \lambda_4) \tag{65}$$

A development paralleling the foregoing could be carried out from the compliance constant point of view (14, p. 241) and would lead to compliance constants defined by

$$\mathbb{C} = \mathbb{F}^{-1} \tag{66}$$

One may investigate the agreement between these constants and those to be predicted from equation (8b) or from an improvement in the approximation implied in it (33, p. 1927):

$$\mathbb{\Sigma}_r = kT\,\mathbb{C} + \frac{h^2}{48\pi^2 kT}\,\mathbb{G} \tag{67}$$

The two mean square amplitudes are thus

$$l^2_{As\text{-}Br} = kT\,C_r + \frac{h^2}{48\pi^2 kT}\,G_r \tag{68}$$

$$l^2_{Br\ldots Br} = kT\,C_R + \frac{h^2}{48\pi^2 kT}\,G_R \tag{69}$$

Results

Although the six equations relating the experimental quantities (λ_i's and l_{ij}'s) to the potential constants ($f_{k,l}$'s) of the general quadratic potential function (Equation 29) provide sufficient means to solve for the six potential constants, it is convenient to represent the solution by a plot such as shown in Figure 13. This plot is useful in that it clearly illustrates the domain of allowed potential constants taking into account the experimental uncertainties associated with the mean amplitudes (Table 14). Each curve is a result of expressing

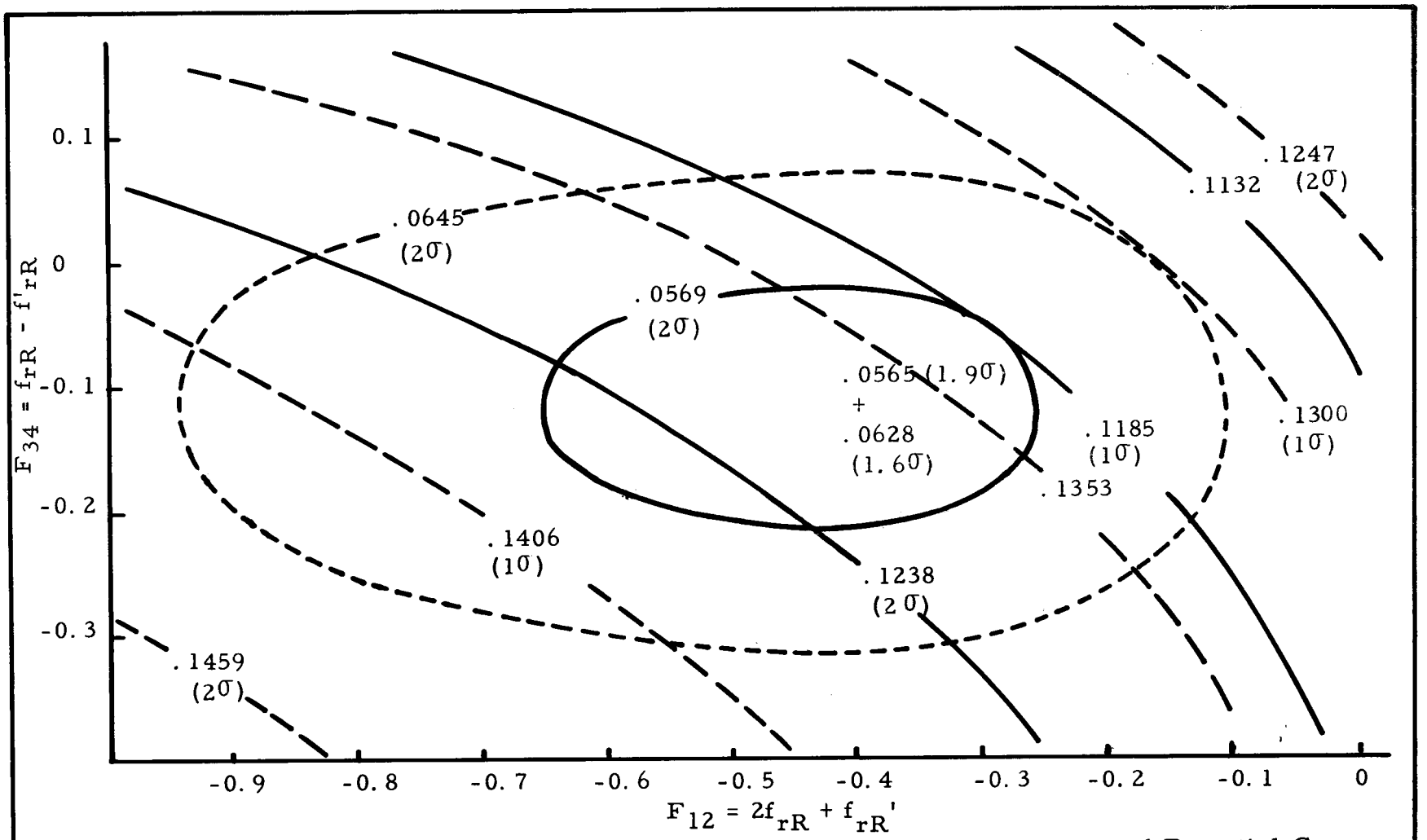

FIGURE 13. Relation between Root-Mean-Square Amplitudes of Vibration and Potential Constants for Arsenic Tribromide. Solid lines are derived from the 370°K Experiment and the Dashed lines from the 473°K Experiment.

the mean amplitudes, l_{As-Br}, and $l_{Br...Br}$, as a function of two of the potential constants, by combining equations (61), (62), (63), and (64) with first equation (59), and second, equation (60). The solid closed contour corresponds to an upper "limit" of l_{As-Br} (.0569 Å) at 370 ° K, and the closed dashed line to an upper limit of l_{As-Br} (.0645 Å) at 473° K. The curves corresponding to the "observed" values (.0479 Å) and (.0555 Å) do not exist in real space and the position of the lower "limiting" values is indicated by a cross (.0565 Å and .0628 Å). The set of solid and dashed curved lines (which are actually parts of closed contours) correspond to $l_{Br...Br}$ at 370° K and 473° K, respectively. The position of "limits" based on the standard errors of Table 14 and on twice these standard errors are also shown for this amplitude.

The domain of allowed potential constants compatible with a given set of mean amplitudes from the diffraction experiment and normal frequencies from vibration spectroscopy, at a given temperature, is given by the intersection of the set of curves corresponding to l_{As-Br} and $l_{Br...Br}$, respectively, and their error "limits." The overlapping of the two domains from each temperature indicates a region of potential constants compatible with all of the experimental data. It was found that at neither temperature does a set of potential constants exist which are compatible with both observed mean amplitudes. Examination of the values of l_{As-Br} at the point indicating the

boundary between real and imaginary space and the values for the curves corresponding to the upper limits at either temperature shows that the elliptical contours for these amplitudes are expanding rapidly for small changes in the amplitudes. On the other hand, the contours for $l_{Br...Br}$ are shrinking for increases in that amplitude, although not at the same rate as for l_{As-Br} (compare the curves corresponding to $l_{Br...Br} = .1132$ and $l_{Br...Br} = .1182$). This indicates that for small increases of $l_{Br...Br}$ above the observed value and for l_{As-Br} above the boundary between real and imaginary space, significant overlap of the allowed potential constant region exists. It should be remarked in passing that the inclusion of small uncertainties in the frequencies, which have been ignored in the foregoing, will permit the same degree of agreement with amplitudes closer in magnitude to those actually observed. This argument is further strengthened by consideration of the error matrix, Table 15. The correlation between l_{As-Br} and $l_{Br...Br}$ is positive indicating that an error which increases one mean amplitude also increases the other. The indication from these considerations is that the probable domain of allowed potential constants (at either temperature) is a region near the origin of Figure 13, leading to small negative values for F_{12} and F_{34}.

In order to obtain a "best" set of potential constants, the observed amplitudes at both temperatures and the observed frequencies

(Table 18) were employed with equations (59) to (64) in a least-squares refinement of the potential constants. The starting model for calculation included the symmetry potential constants from the simple central force field of Table 21. The results of this calculation are given in the same table. In Table 20 is given a comparison between the observed amplitudes and frequencies and the calculated values based on the least-squares results. The least-squares fit for the frequencies is good, especially when cognizance is taken of the large uncertainty in ν_1: this frequency is not directly observed and is estimated from the combination band $\nu_1 + \nu_4$ observed at 382 cm^{-1} (31, p. 117).

Also given in Table 21 is the inverse **F**, or compliance matrix (equation 66). The values for the potential constants for the internal coordinates used (equation 52) are shown in Table 19 along with the corresponding compliance constants. The values from the simple central force field (all cross terms in equation (52) equal to zero) are also given in the table for comparison, together with the "observed" values for the diagonal compliance matrix elements based on the approximation (equation 67) discussed in the section above.

TABLE 17. Values of Constants used in Vibrational Potential Function Determinations .

$\times 10^{22}$		$\times 10^{40}$	370°K	473°K		370°K	473°K
G_r	1.5576	Δ_1	.1912	.2359	$a \times 10^{42}$	1.7244	1.3614
G_{rr}	-0.1418	Δ_2	.8736	1.1081	$a' \times 10^{42}$	1.7294	1.3638
G_R	1.5073	Δ_3	.2028	.2507	$b \times 10^{24}$	11.451	14.636
G_{RR}	0.3768	Δ_4	1.4779	1.8806	$b' \times 10^{24}$	20.611	26.345
G_{rR}	0.5773						
$G_{rR'}$	0.0000						

G's calculated on the basis of $\mu_{As} = 8.0401 \times 10^{21}$ gm^{-1}, $\mu_{Br} = 7.5364 \times 10^{21}$ gm^{-1}.

TABLE 18. Fundamental Vibrational Frequencies of Arsenic Tribromide (in cm^{-1}) (31).

Mode	$\nu_2(A_1)$	$\nu_2(A_1)$	$\nu_3(E)$	$\nu_4(E)$
Frequency	284[a]	128	275	98

(a) Estimated

TABLE 19. Potential and Compliance Constants in Internal Coordinates .

	LS	CF		LS	CF	Observed
f_r *	1.69	1.67	C_r +	0.60	0.61	$.42 \pm .16$
f_{rr}	.23	.14	C_{rr}	-0.07	-0.05	
f_R	.42	.41	C_R	2.52	2.52	$2.61 \pm .43$
f_{RR}	.07	.06	C_{RR}	-0.35	-0.35	
f_{rR}	-.03	0	C_{rR}	0.02	0	
$f_{rR'}$	-.05	0	$C_{rR'}$	0.05	0	

LS: Results from least-squares analysis
CF: Calculated on the basis of a simple central force field

* in Millidynes/Å
\+ in Å/Millidynes

TABLE 20. Comparison of the Calculated and Observed Frequencies (in cm^{-1}) and Root-Mean-Square Amplitudes (in Å) Based on the Potential Constants gotten from the Least-Squares Refinement of the Vibrational Potential Function.

	Calc.	Obs.	Diff. (Percent)
$\nu_1 (A_1)$	297	284 [a]	+4.6
$\nu_2 (A_2)$	128	128	.0
$\nu_3 (E)$	270	275	-1.8
$\nu_4 (E)$	96	98	-2.0
At 370°K			
l_{As-Br}	$.058_5$	$.048_0$	+21.9
$l_{Br...Br}$	$.114_0$	$.113_0$	+1.1
At 473°K			
l_{As-Br}	$.065_0$	$.055_5$	+17.1
$l_{Br...Br}$	$.129_0$	$.135_5$	-4.6

(a) Estimated

TABLE 21. Potential Constant Matrices for Arsenic Tribromide.

+ Symmetry Potential Constants from Least-Squares Analysis					# Symmetry Compliance Matrix from Least-Squares Analysis				
F_s*	1	2	3	4	C_s	1	2	3	4
1	2.15	-.12			1	.46	.10		
2	-.12	.55			2	.10	1.82		
			1.47	.02	3			.68	-.03
			.02	.35	4			-.03	2.88

+ Symmetry Potential Constants from Simple Central Force Field					# Symmetry Compliance Matrix from Simple Central Force Field				
F_s	1	2	3	4	C_s	1	2	3	4
1	(1.95)[a]	0			1	.51	0		
2	0	(.55)[a]			2	0	1.82		
3			1.53	0	3			.66	0
4			0	.35	4			0	2.88

(a) Based on $\nu_1 = 290$. $\nu_1 = 284$ provided for no real solution

* Indexing is given in terms of row and column of the matrix, i.e. $F_{12} = -.12$ in F_s

+ in Millidynes/Å

in Å/Millidynes

SUMMARY

The molecular structure of arsenic tribromide was determined with high accuracy. The molecular parameters r_{As-Br}, $r_{Br...Br}$ and $\angle B_r\text{-}A_s\text{-}B_r$ have values that agree well with previous, but much earlier, results (1, p. 67). The standard errors associated with the determination and evaluation of all the molecular parameters show that the values of the internuclear distances are probably accurate to within 0.1 percent, and the root-mean-square amplitudes of vibration to about four percent ($l_{Br...Br}$) and nine percent (l_{As-Br}).

An expected increase in the mean amplitudes as a result of an increase in temperature was demonstrated: the curves resulting from analyses of the experimental intensity data clearly show the effect of increased mean amplitudes. The least-squares results from the structure work at the two temperatures agree well with the expected proportionality of the mean-square amplitudes with temperature.

The uncertainites in the determination of the mean amplitudes preclude any precise determination of the vibrational potential function, but the results strongly indicate the off diagonal terms of the F matrix are small and probably negative, suggesting that a simple central force field can be applied with confidence to arsenic tribromide.

BIBLIOGRAPHY

1. Allen, P.W. and L. E. Sutton. Tables of interatomic distances and molecular configurations obtained by electron diffraction in the gas phase. Acta Crystallographica 3:46-72. 1950.

2. Bartell, L.S. and L.O. Brockway. The calibration of photographic emulsions for electron diffraction investigations. The Journal of Applied Physics 24:656-657. 1953.

3. Bartell, L.S. and K. Kuchitsu. Significance of bond lengths determined by electron diffraction. Journal of the Physical Society of Japan 17 (Supplement 2):20-22. 1962.

4. Bastiansen, O., O. Hassel, and Eilif Risberg. The Oslo electron diffraction units for gas work. Acta Chemica Scandinavica 9:232-238. 1955.

5. Bastiansen, Otto, Lise Hedberg and Kenneth Hedberg. Reinvestigation of the molecular structure of 1,3,3,7-cyclooctatetraene by electron diffraction. The Journal of Chemical Physics 27:1311-1317. 1957.

6. Bastiansen, O. The sector microphotometer method for location of H_2 in gas molecules. Acta Chemica Scandinavica 9:815-821. 1955.

7. Bewilogua, L. Uber die inkoharente Streuung der Rontgenstrahlen. Physikalische Zeitscrift 32:470-474. 1931.

8. Block, F. Auf Theorie des Austauschproblem und der Remanenzerscheinung der Ferromagnetika. Zeitschrift fur Physik. 74:295-335. 1935.

9. Brockway, L.O. Electron diffraction by gas molecules. Reviews of Modern Physics 8:231-266. 1936.

10. Crawford, Roger Allen. An electron diffraction investigation of the molecular structure of gaseous pentafluorosulfur hypofluorite (SOF_6). PhD thesis. Corvallis, Oregon State University, 1959. 152 numb. leaves.

11. Debye, P. Elektronen Interferenzen an Leichten Molekulen nach dem Sektorverfahren. Physikalische Zeitschrift. 40:404-406. 1939.

12. Debye, P. The influence of intramolecular atomic motion on electron diffraction diagrams. The Journal of Chemical Physics 9:55-60. 1940.

13. Decius, J.C. Classical limit of mean thermal vibration amplitudes. The Journal of Chemical Physics 21:1121. 1953.

14. Decius, J.C. Compliance matrix and molecular vibrations. The Journal of Chemical Physics 38:241-248. 1963.

15. Decius, J.C. The use of isotopic molecules for the complete determination of force constants. I. Linear molecules. The Journal of Chemical Physics 20:511-516. 1962.

16. Freeman, A.J. A study of the Compton scattering of x-rays: Ne, Cu^{+}, Cu, and Zn^{+2}. Acta Crystallographica 12:929-932. 1959.

17. Freeman, A.J. X-ray incoherent scattering functions for non-spherical charge distributions: N, N^{-}, O, O^{+}, O^{+2}, O^{+3}, F, F^{-}, Si^{+4}, Si^{+3}, Si, and Ge. Acta Crystallographica 12:274-281. 1959.

18. Glasstone, Samuel. Theoretical chemistry. Princeton, D. Van Nostrand, 1944. 515p.

19. Glauber, R. and V. Schomaker. The theory of electron diffraction. Physical Review 89:667-671. 1953.

20. Hanson, Harold P. Experimental determination of Br f values by electron diffraction. Acta Chemica Scandinavica 15:952-954. 1961.

21. Hanson, Harold P. Unpublished calculations of atomic scattering factors. Austin, Texas. University of Texas. Department of Physics, (1963).

22. Hedberg, Kenneth, and Machio Iwasaki. Effect of temperature on the structure of gaseous molecules. Molecular structure of PCl_3 at 300°K and 505°K. The Journal of Chemical Physics 36:589-594. 1962.

23. Hedberg, Kenneth, and Machio Iwasaki. Potential constants of PCl_3 from amplitudes of vibration and normal vibrations. The Journal of Chemical Physics 36:594-598. 1962.

24. Ibers, J.A. Atomic scattering amplitudes for electron diffraction. Acta Crystallographica 7:405-408. 1954.

25. Ibers, J.A. Atomic scattering factors. In: International tables for x-ray crystallography, vol. 3. Birmingham, England, Kynock Press, 1963. p. 201-227.

26. Ino, T. Studies on the radial distribution analysis in diffraction methods. III. Extrapolation of intensity data to small scattering angle. Journal of the Physical Society of Japan 16:2239-2245. 1961.

27. James, R. W. Uber der ein Fluss der Temperatur auf die Streuung der Rontgenstrahlen durch Gasmolekule. Physikalsche Zeitschrift 33:737-754. 1932.

28. Karle, Isabella Lugoski, and Jerome Karle. Internal motion and molecular structure studies of electron diffraction. II. Interpretation and method. The Journal of Chemical Physics 18:957-962. 1950.

29. Karle, I. Lugoski, D. Hoober, and J. Karle. An improved microphotometer trace of radially symmetric patterns. The Journal of Chemical Physics 15:765. 1947.

30. Kuchitsu, Kozo. Electron diffraction investigation on the molecular structure of n-butane. The Chemical Society of Japan. Bulletin 32:748-769. 1959.

31. Miller, Foil A. and William K. Baer. The vibrational spectra of vanadium oxytribromide and arsenic tribromide. Spectrochimica Acta 17:112-120. 1961.

32. Moore, Walter S. Physical chemistry, 2d ed. New York, Prentice Hall, 1955. 633p.

33. Morino, Yonezo, et al. The mean amplitudes of thermal vibrations in polyatomic molecules. II. An approximate method for calculating mean-square amplitudes. The Journal of Chemical Physics 21:1927-1933. 1953.

34. Morino, Yonezo, Yasushi Nakanura, and Takao Ijima. Mean-square amplitudes and force constants of tetrahedral molecules. I. Carbon tetrachloride and germanium tetrachloride. The Journal of Chemical Physics 32:643-652. 1960.

35. Rockholt, Celia Rose. An electron diffraction investigation of the molecular structure of gaseous fluorine flourosulfonate (SO_3F_2). Master's thesis. Corvallis, Oregon State University, 1962. 49 numb. leaves.

36. Shibata, Shuzo. Electron diffraction study on the molecular structure of chlorine. Journal of the Physical Society of Japan 17 (Supplement 2):34-36. 1962.

37. Waser, Jurg, and Verner Schomaker. The Fourier inversion of diffraction data. Reviews of Modern Physics 25:671-690. 1953.

38. Wilson, E. Bright Jr., J.C. Decius and Paul C. Cross. Molecular vibrations. New York, McGraw Hill, 1955. 388p.